ADVANCED MATERIALS

Supporting Information

for *Adv. Mater.*, DOI 10.1002/adma.202211337

Activatable Graphene Quantum-Dot-Based Nanotransformers for Long-Period Tumor Imaging and Repeated Photodynamic Therapy

Yuqi Yang, Baolong Wang, Xu Zhang, Hongchuang Li, Sen Yue, Yifan Zhang, Yunhuang Yang, Maili Liu, Chaohui Ye, Peng Huang and Xin Zhou**

WILEY-VCH

Supporting Information

Activatable Graphene Quantum Dots-Based Nano-Transformers for Long-period Tumor Imaging and Repeated Photodynamic Therapy

Yuqi Yang,† Baolong Wang,† Xu Zhang, Hongchuang Li, Sen Yue, Yifan Zhang, Yunhuang Yang, Maili Liu, Chaohui Ye, Peng Huang and Xin Zhou**

Dr. Y. Yang, B. Wang, X. Zhang, H. Li, S. Yue, Prof. Y. Yang, Prof. M. Liu, Prof. C. Ye, and Prof. X. Zhou
Key Laboratory of Magnetic Resonance in Biological Systems, State Key Laboratory of Magnetic Resonance and Atomic and Molecular Physics, National Center for Magnetic Resonance in Wuhan, Wuhan Institute of Physics and Mathematics, Innovation Academy for Precision Measurement Science and Technology, Chinese Academy of Sciences–Wuhan National Laboratory for Optoelectronics, Huazhong University of Science and Technology, Wuhan, 430071, China
Optics Valley Laboratory, Wuhan, Hubei, 430073, China
University of Chinese Academy of Sciences, Beijing, 100049, China
E-mail: xinzhou@wipm.ac.cn

Dr. Y. Zhang, Prof. P. Huang
Marshall Laboratory of Biomedical Engineering, International Cancer Center, Laboratory of Evolutionary Theranostics (LET), School of Biomedical Engineering, Health Science Center, Shenzhen University, Shenzhen, 518060, China
E-mail: peng.huang@szu.edu.cn

Table of Contents

Materials and Instruments

Materials. 8-Armed-PEG10000-NH_2 (MPEG-NH_2) and Boc-NH-PEG2000-NH_2 were purchased from Ponsure Biotech, Inc (Shanghai, China). 4,4',4",4"'-(Porphine-5,10,15,20-tetryl) tetrakis(benzoic acid) and 1-Adamantanecarbonyl chloride (Ad) were purchased from Aladdin Reagent (Shanghai, China). Beta-cyclodextrin was purchased from Sinopharm (Beijing, China). All purchased chemicals were used directly without further purification. Manganese(II) *meso*-tetra(4-carboxyphenyl) porphyrin (Mn-TCPP)[1], GQDs[2], and 6-Mono-tosyl-β-cyclodextrin (6-OTs-β-CD)[3] were prepared according to literature reported method. Materials for cell culture, including PBS, Ham's F-12 medium (F12K), MEM, DMEM, and fetal bovine serum (FBS) were purchased from Boster Biological Technology Co. Ltd. (Wuhan, China). Annexin V-fluo647/propidium iodide (PI) apoptosis detection kit was purchased from Solarbio Scientific Ltd. (Beijing, China). Singlet oxygen detection kit and calcein acetoxymethyl ester (Calcein AM)/propidium iodide (PI) detection kit were purchased from BioRab Technology Co. Ltd. (Beijing, China).

Instruments. A JEM-2100 transmission electron microscope (Jeol Ltd., Tokyo, Japan) and a Zetasizer Nano-ZS particle sizer (Malvern Instruments, UK) were used for the characterization of nanoparticles. UV-vis absorption spectra were recorded on an Evolution 220 spectrophotometer (Thermo fisher scientific). Fluorescence spectra were recorded at room temperature on an Edinburgh FS5 fluorescence spectrophotometer. Confocal fluorescence images were obtained by a laser scanning confocal microscope Nikon A1 (Nikon, Tokyo, Japan). Fluorescence imaging of mice was performed on a PerkinElmer multi-channel optical imaging system (Waltham, USA). T_1-weighted magnetic resonance imaging (MRI) was performed by a 7 T small animal horizontal bore MRI scanner (Bruker BioSpec 70/20 USR, Bruker, Ettlingen, Germany).

Synthesis Section

Synthesis of GQD-PEG-Ad. Adamantyl-functionalized PEG (NH_2-PEG-Ad) was synthesized according to previous literature[4]. Briefly, 1-adamantane carbonylchloride (25 mg, 0.125 mmol) was dissolved in 5 mL anhydrous dichloromethane (DCM) and kept in an ice bath. Next, Boc-PEG-NH_2 (50 mg, 0.025 mmol, Mw 2000 Da) and triethylamine (10 μL) were dissolved in 5 mL DCM and added dropwise within 30 min. And then the mixture was stirred at room temperature for 12 h. After the reaction was completed, the DCM was removed by decompression rotary evaporator, and the obtained residue was dissolved in 5 mL DI water by ultrasound. Subsequently, the solution was centrifuged to remove 1-adamantane carboxylic acid. The supernatant was dialyzed against DI water for 48 h (MWCO: 1 kDa). Boc-PEG-Ad was obtained after freeze-drying and characterized by nuclear magnetic resonance (^{1}H-NMR).

Next, Boc-PEG-Ad was dissolved in TFA/DCM solution and stirred at room temperature for 6 h to remove Boc. The solution was removed by a decompression rotary evaporator. Meanwhile, N-hydroxysuccinimide (NHS, 150 mg, 1.3 mmol) and 1-(3-Dimethylaminopropyl)-3-ethylcarbodiimide hydrochloride (EDC, 248 mg, 1.3 mmol) were added to GQDs solution (10 mg, 10 mL). After 2 h stirring at room temperature, NH_2-PEG-Ad (50 mg) and triethylamine (50 μL) were added. The mixture was stirred for another 48 h at room temperature. The produced GQD-PEG-Ad solution was purified by dialysis against DI water (MWCO, 6000 Da). Finally, the synthesized GQD-PEG-Ad was lyophilized and stored in the refrigerator (the grafting rate of PEG was 47%).

Synthesis of 8-armed PEG-CD. 8-Armed-PEG-cyclodextrin (MPEG-CD) was synthesized according to previous literature[5]. To a solution of 8-Armed-PEG-NH_2 (50 mg, 5 μmol, Mw 10000 Da) in 5 mL DMSO, 6-OTs-β-CD (258 mg, 0.2 mmol) was added. After reacting at 50 ℃ for 3 days, the mixture was purified by dialysis against DI water (MWCO, 3500 Da).

After dialysis, the reaction mixture was filtrated to remove the unreacted 6-OTs-β-CD as a white precipitate. Finally, the synthesized MPEG-CD was lyophilized and stored in the refrigerator (yield 56%).

Synthesis of RGD-PEG-Ad. 1-adamantane carbonylchloride (25 mg, 0.125 mmol) was dissolved in 5 mL anhydrous dichloromethane (DCM) and kept in an ice bath. Next, NH_2-PEG-COOH (50 mg, 0.025 mmol, Mw 2000 Da) and triethylamine (10 μL) were dissolved in 5 mL DCM and added dropwise within 30 min. And then the mixture was stirred at room temperature for 12 h. After the reaction was completed, the DCM was removed by decompression rotary evaporator, and the obtained residue was dissolved in 5 mL DI water by ultrasound. The solution was centrifuged to remove 1-adamantane carboxylic acid. The supernatant was lyophilized and dissolved in 5 mL PBS (pH 7.4).

Simultaneously, 1-(3-Dimethylaminopropyl)-3-ethylcarbodiimide hydrochloride (EDC, 19.2 mg, 0.1 mmol) and N-hydroxysuccinimide (NHS, 11.5 mg, 0.1 mmol) were added to PBS solution. After 2 h stirring at room temperature, c(RGDyk) (18.57 mg, 0.03 mmol) was added. The mixture was stirred for another 48 h at room temperature. The produced RGD-PEG-Ad solution was purified by dialysis against DI water (MWCO, 1000 Da). Finally, the synthesized RGD-PEG-Ad was lyophilized and stored in the refrigerator (yield 60%).

Preparation of GQD NT. To a PBS (pH 7.4) or DI water solutions of GQD-PEG-Ad (1 mg/mL, 5 ml), corresponding amount PBS or DI water solutions of MPEG-CD (1 mg/mL, 10 mL) was added dropwise under vigorous stirring, followed by stirring the mixture for 24 h at 25 ℃. Then RGD-PEG-Ad PBS solution (1 mg/mL, 0.4 mL, 10%) was added dropwise and stirred for another 3 h. At last, the GQD NT solution was ultrafiltered to remove excess unassembled modules.

Preparation of TCPP and Mn-TCPP@GQD NT. TCPP or Mn-TCPP (0.01 mmol) was dissolved in 10 mL DMSO and added in DI water solution of GQD-PEG-Ad (1 mg/mL, 5 mL)

dropwise under vigorous stirring at 0 ℃. The mixture was further stirred overnight in dark at room temperature. And then DI water solution of MPEG-CD (1 mg/mL, 10 mL) was added dropwise, followed by stirring the mixture for 24 h at 25 ℃. The solution was purified by dialysis against DI water (MWCO, 50 KDa). After dialysis, the reaction mixture was centrifuged to remove the unloaded TCPP or Mn-TCPP. Then RGD-PEG-Ad PBS solution (1 mg/mL, 0.4 mL, 10%) was added dropwise and stirred for another 3 h. At last, the TCPP or Mn-TCPP@GQD NT solution was ultrafiltered to remove unassembled modules.

Characterization of GQD NT. The percentage of GQD in GQD NT was calculated by weighing the dried powder of GQD-PEG-Ad before self-assembly and GQD NT after dialysis. The drug loading capacity of GQD NT was measured by ultraviolet-visible (UV-vis) standard curve method of DMSO solution of TCPP and Mn-TCPP. Briefly, TCPP@GQD NT or Mn-TCPP@GQD NT dried powder was completely dissolved in pure DMSO, and then the UV-vis absorption of DMSO solution was measured by UV-vis spectrometer. And TCPP or Mn-TCPP content was calculated using the standard curve.

To dynamically observe the morphological changes induced by mild acidity, the GQD NT were first dispersed in 4 mL of phosphate-buffered saline (PBS, pH 7.4), and then the pH of the suspension was adjusted by continuously adding 0.1 M HCl solution. The morphological and hydrodynamic size changes of the GQD NT were characterized by transmission electron microscopy (TEM) and dynamic light scattering (DLS) respectively. To evaluate the long-term stability of the GQD NT, the TCPP@GQD NT and Mn-TCPP@GQD NT were dispersed in a PBS solution (pH 7.4), followed by UV-vis and fluorescence analysis every day for a determined time period.

Measurement of the Photothermal Effect. To evaluate the photothermal performance of GQD NT, 1 mL of the DI H_2O, GQD, GQD NT, TCPP@GQD NT, and Mn-TCPP@GQD NT suspensions with 3 mg/ml GQD NT (corresponding to concentration of *in vivo* photodynamic

therapy) were placed in 1.5 mL tubes. Then, the suspensions were irradiated by a 650 nm laser (100 mW/cm^2), and the temperature changes were recorded by a thermal imager.

Measurement of relaxation rate. MR imaging (MRI) of Mn-TCPP@GQD NT solutions with different Mn concentrations (0.006, 0.012, 0.023, 0.046 mM) was performed on 7T Bruker BioSpec 70/20 USR system, RARE and MSME sequences were used for collecting MRI images and fitting the relaxation times.

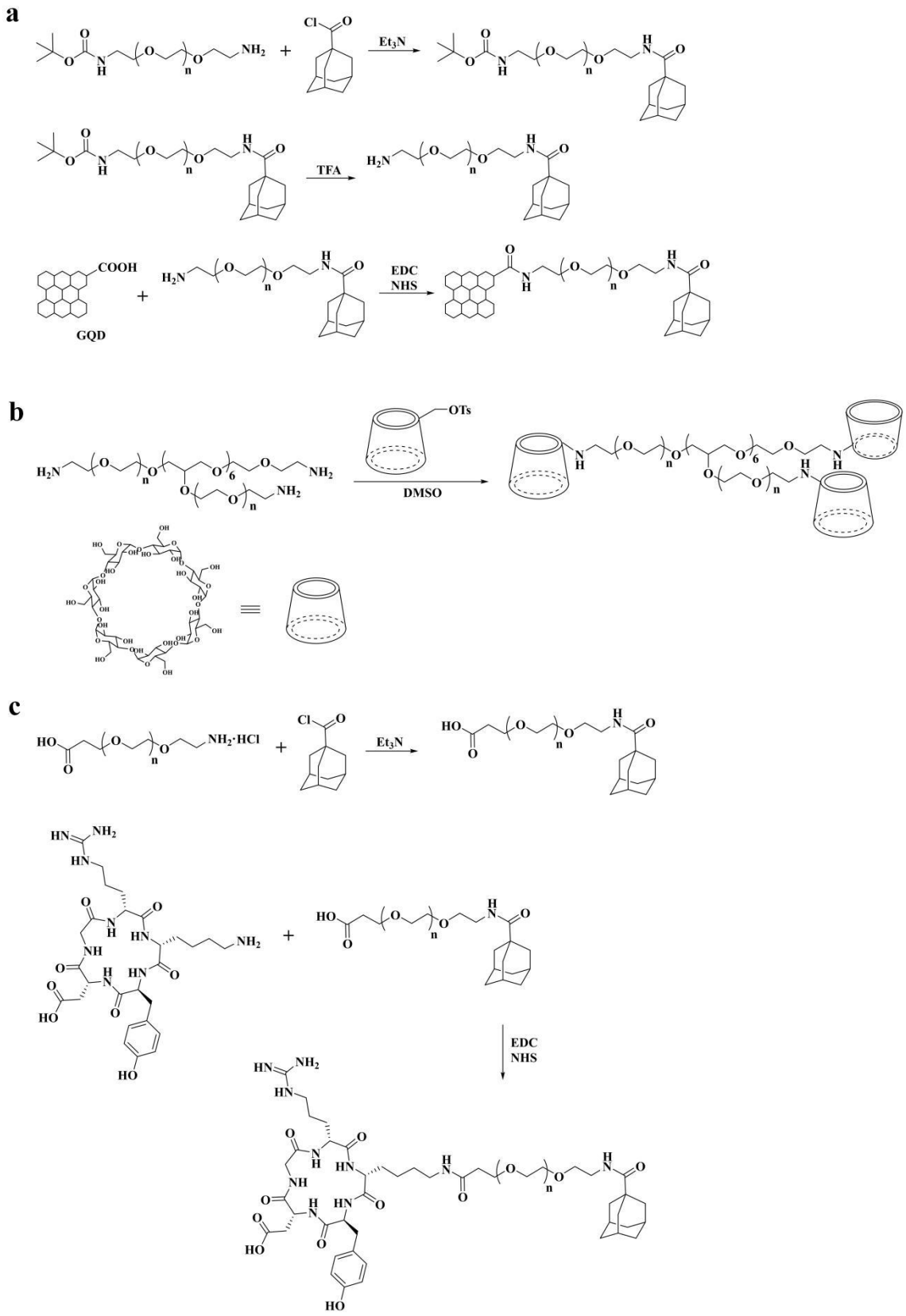

Figure S1. Synthetic routes of (a) GQD-PEG-Ad, (b) 8-armed PEG-CD, and (c) RGD-PEG-Ad.

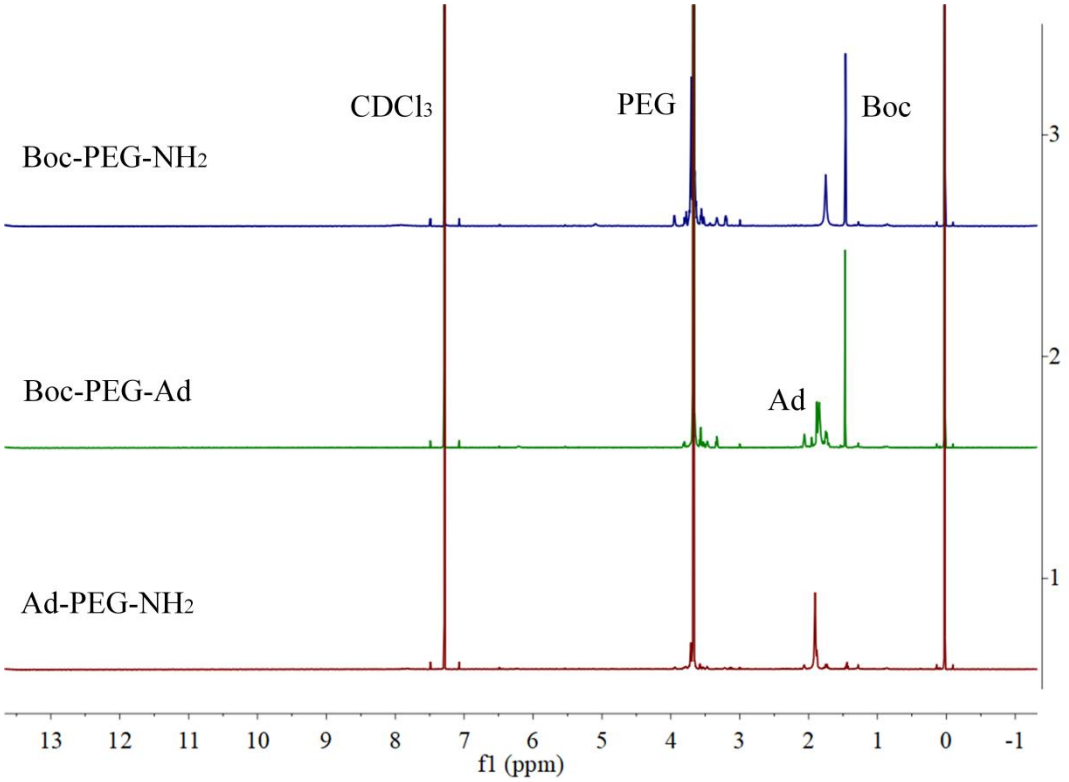

Figure S2. ^{1}H NMR spectra of Boc-PEG-NH_2, Boc-PEG-Ad, and Ad-PEG-NH_2 in $CDCl_3$.

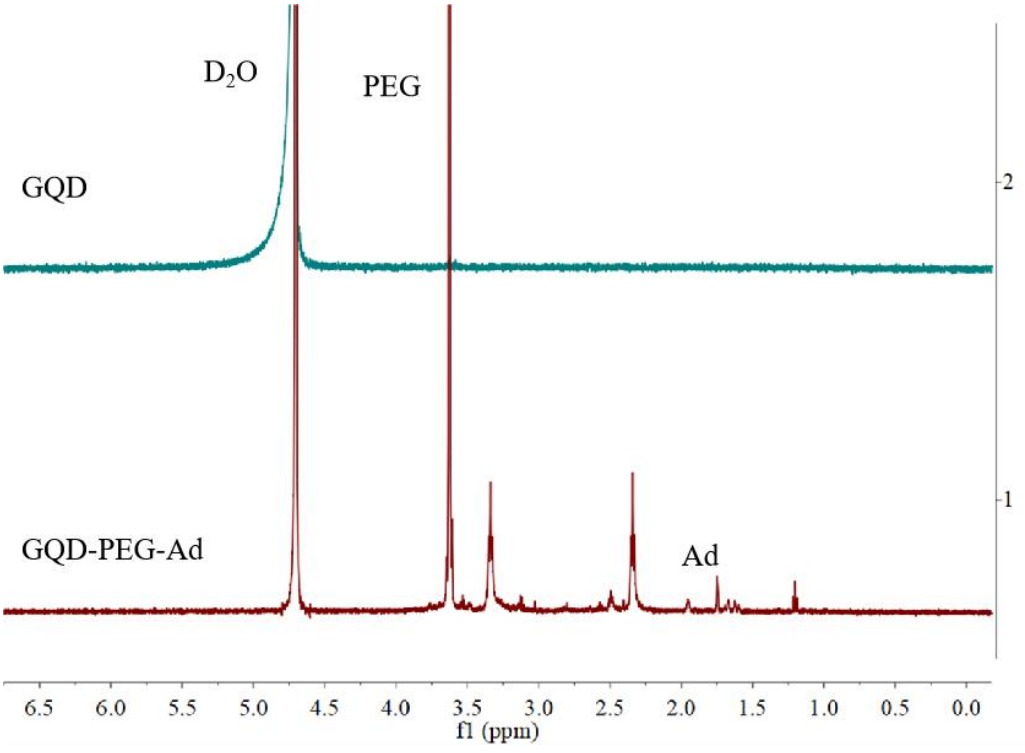

Figure S3. ^{1}H NMR spectra of GQD and GQD-PEG-Ad in D_2O.

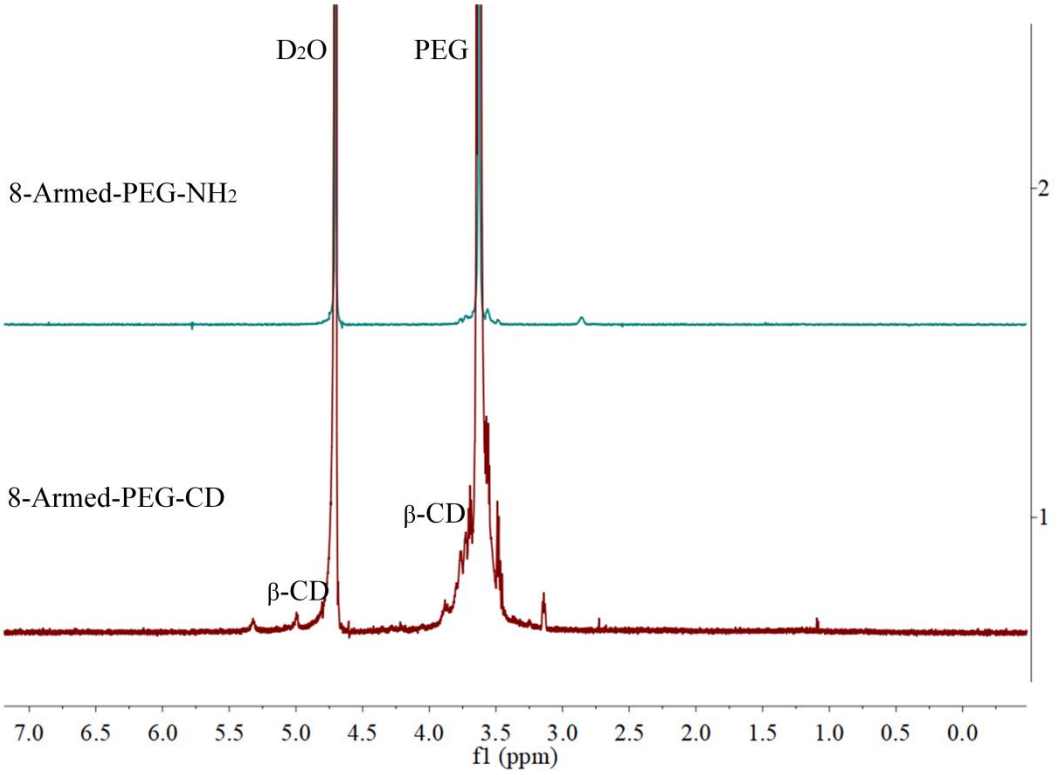

Figure S4. ^{1}H NMR spectra of 8-armed PEG-NH_2 and 8-armed PEG-CD in D_2O.

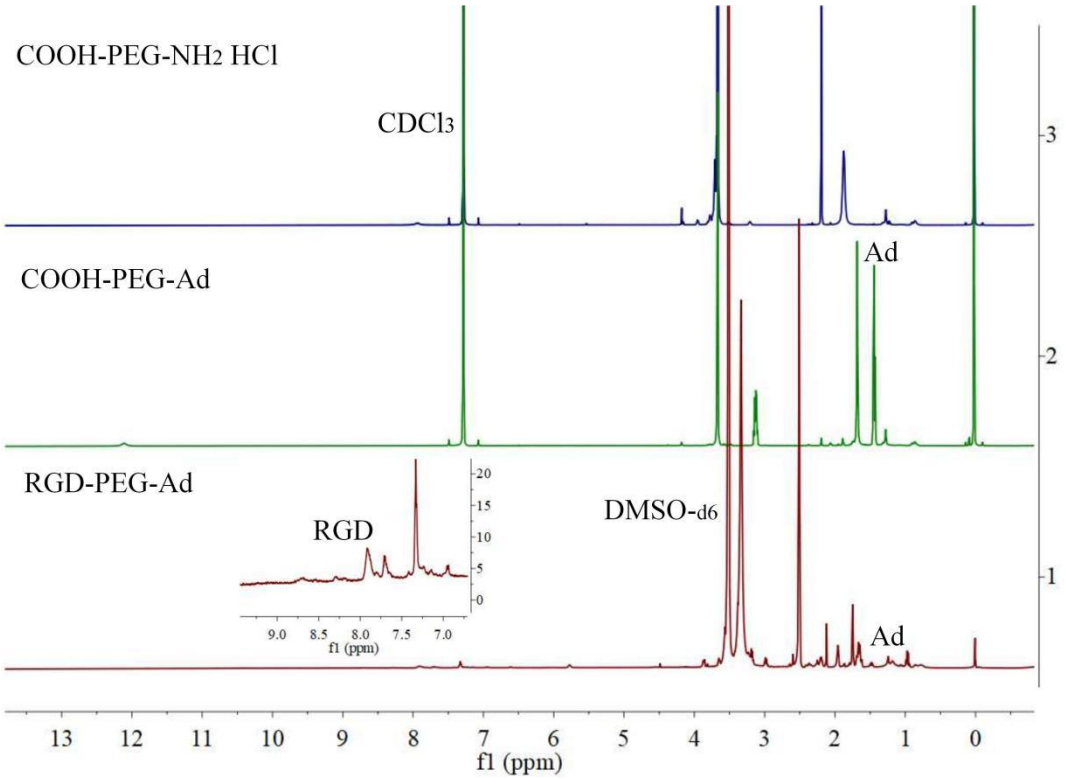

Figure S5. ^{1}H NMR spectra of COOH-PEG-NH_3Cl, COOH-PEG-Ad in $CDCl_3$, and RGD-PEG-Ad in DMSO-d_6.

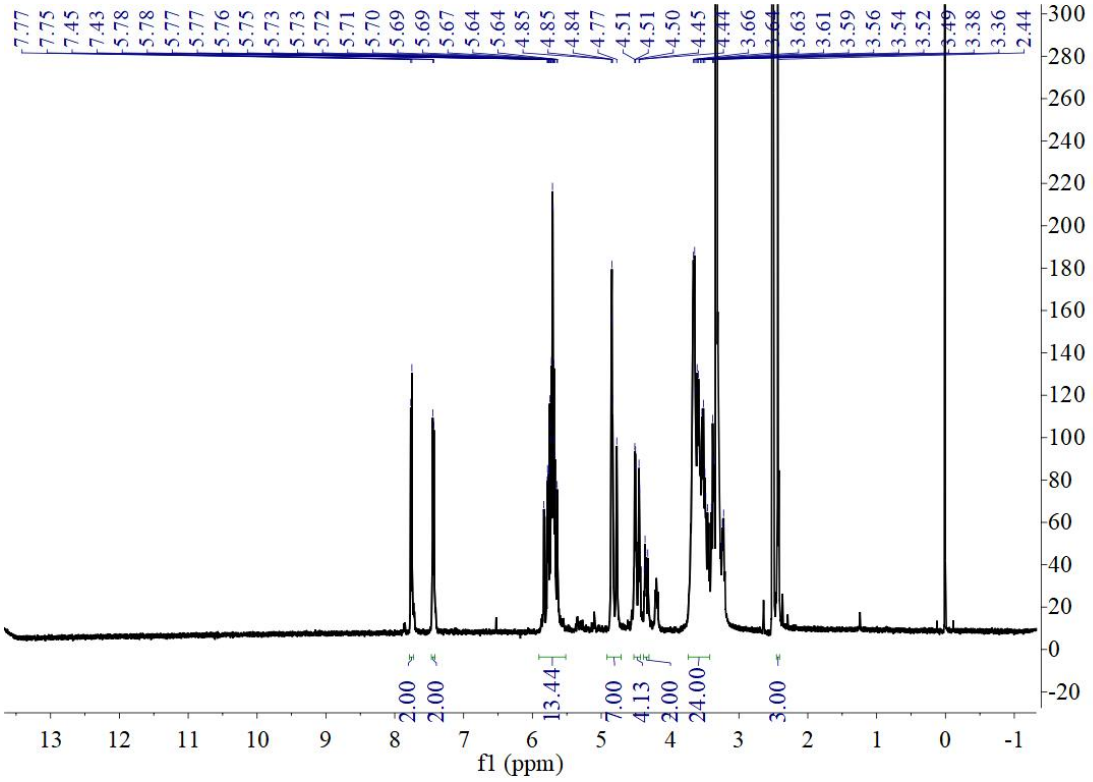

Figure S6. ^{1}H NMR spectrum of Mono-6-deoxy-6-(*p*-tolylsulfonyl)-*β*-cyclodextrin in DMSO-d_6.

Mono-6-deoxy-6-(p-tolylsulfonyl)-β-cyclodextrin: ^{1}H NMR (500 MHz, DMSO) δ 7.76 (d, J = 8.3 Hz, 2H), 7.44 (d, J = 8.3 Hz, 2H), 5.85 – 5.62 (m, 14H), 4.83 (dd, J = 22.0, 17.1 Hz, 7H), 4.53 – 4.42 (m, 4H), 4.39 – 4.31 (m, 2H), 3.75 – 3.42 (m, 24H), 3.42-3.17 (m, overlaps with HOD), 2.44 (s, 3H).

Characterization Section

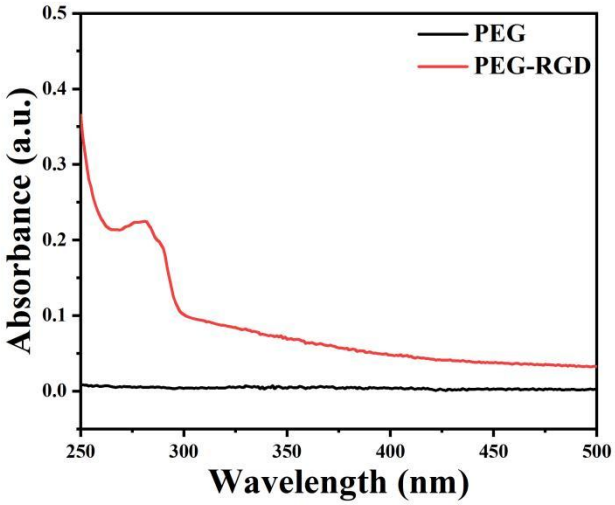

Figure S7. UV absorption of COOH-PEG-NH_2 and RGD-PEG-Ad.

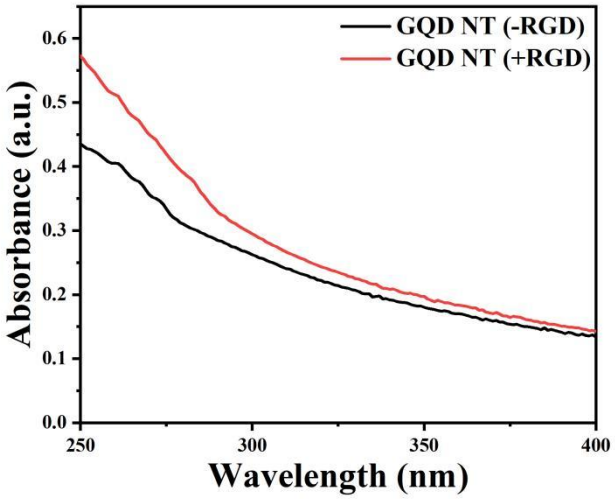

Figure S8. UV absorption of GQD NT with or without RGD.

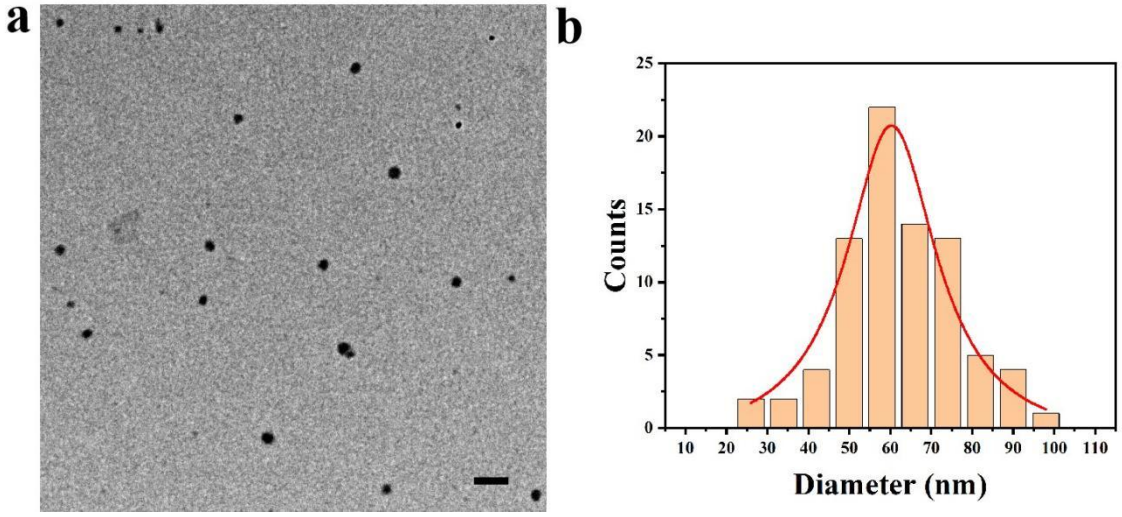

Figure S9. (a) TEM image of GQD NT. Scale bar, 200 nm. (b) Size distribution counted by TEM.

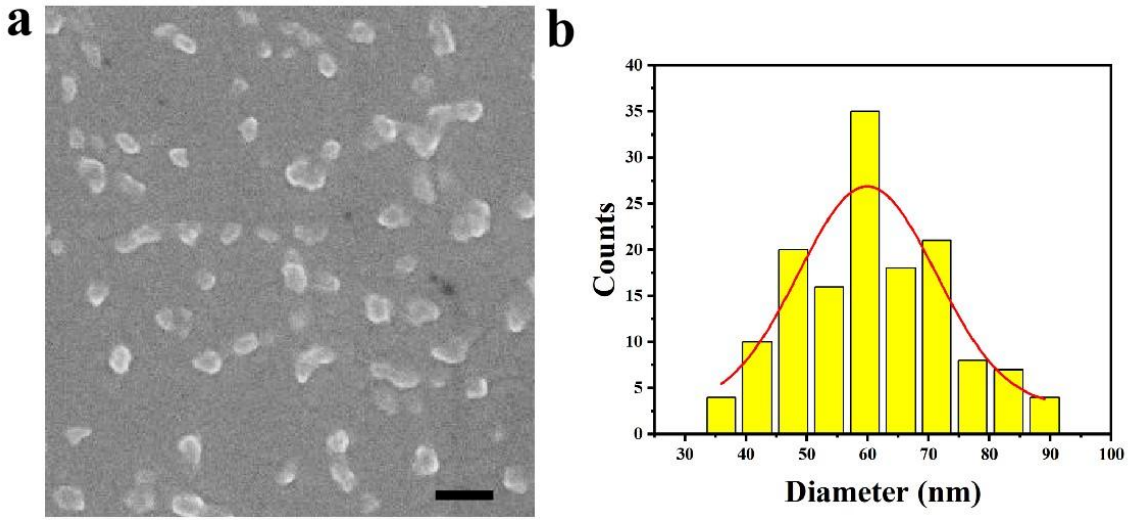

Figure S10. (a) SEM image of GQD NT. Scale bar, 200 nm. (b) Size distribution counted by SEM.

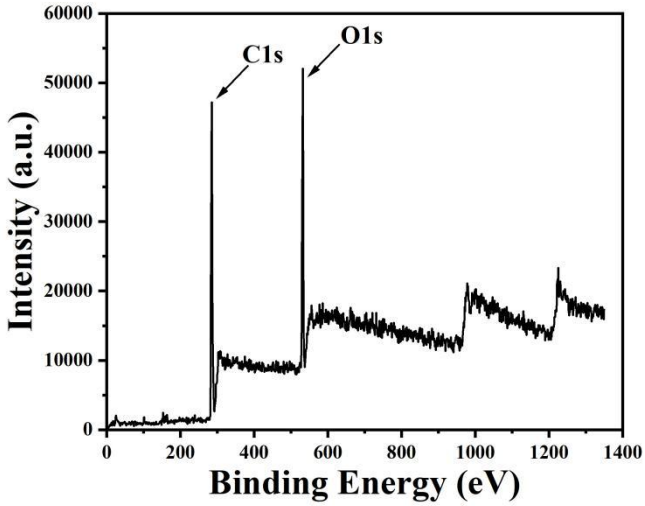

Figure S11. XPS spectrum of GQD NT.

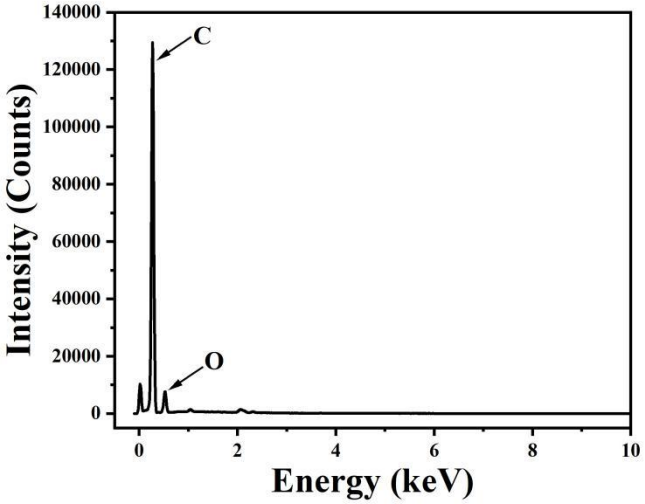

Figure S12. EDS pattern of GQD NT.

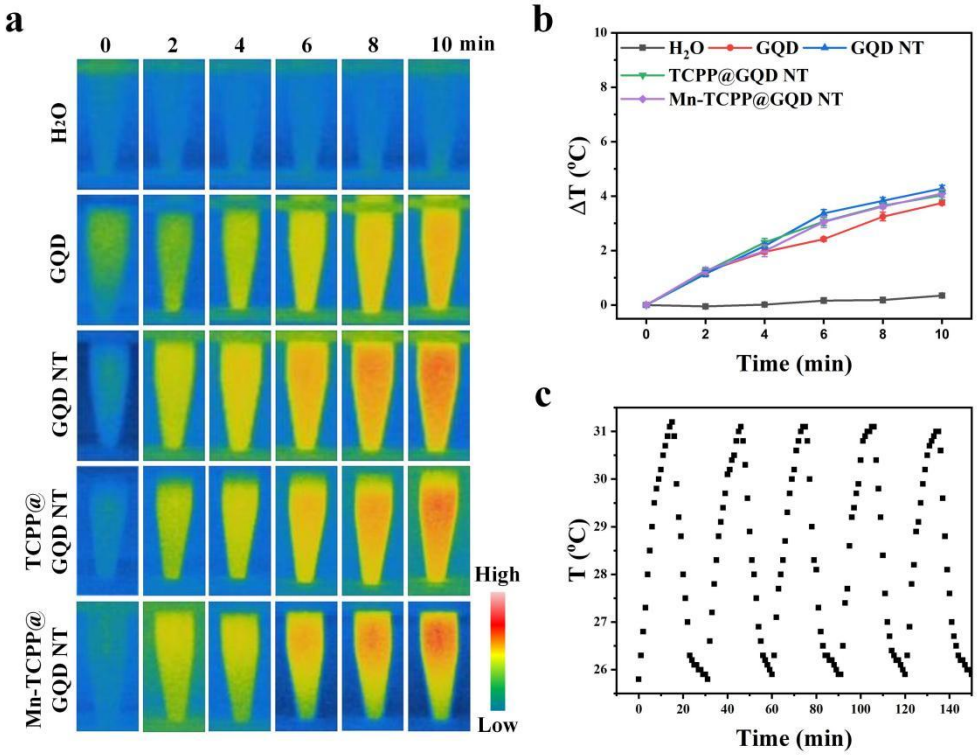

Figure S13. Photothermal conversion effect of GQD NT. (a) Photothermal conversion images and (b) the corresponding temperature changes of PBS, GQD, GQD NT, TCPP@GQD NT, and Mn-TCPP@GQD NT by a 650 nm laser (100 mW/cm^2) for a duration of 10 min. (c) Temperature changes GQD NT during the five laser on/off cycles. The concentration of the solutions is the same as that used in PDT treatments *in vivo*.

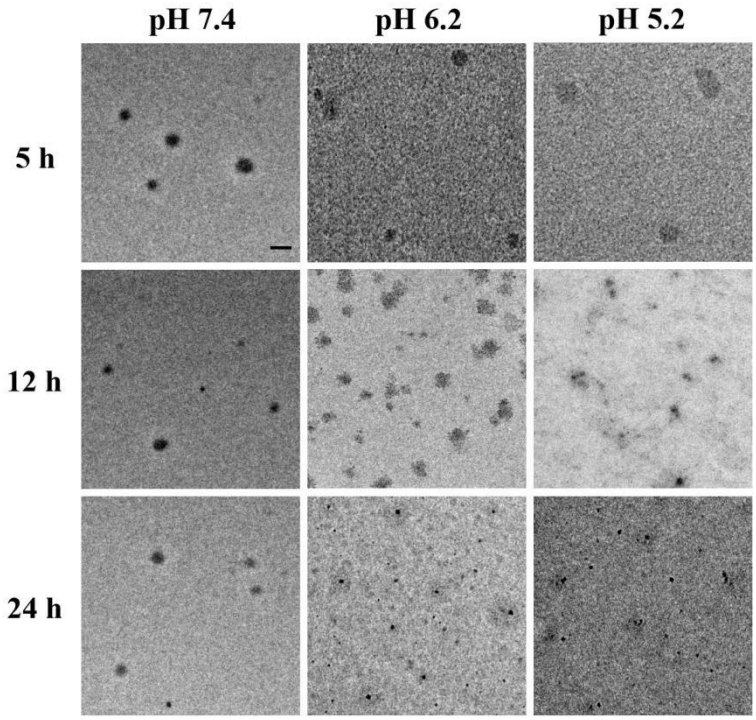

Figure S14. TEM results illustrate the morphological changes of GQD NT induced by mild acidity. GQD NT in pH 7.4, 6.2 and 5.2 were characterized by TEM at different incubation time. Scale bar, 100 nm.

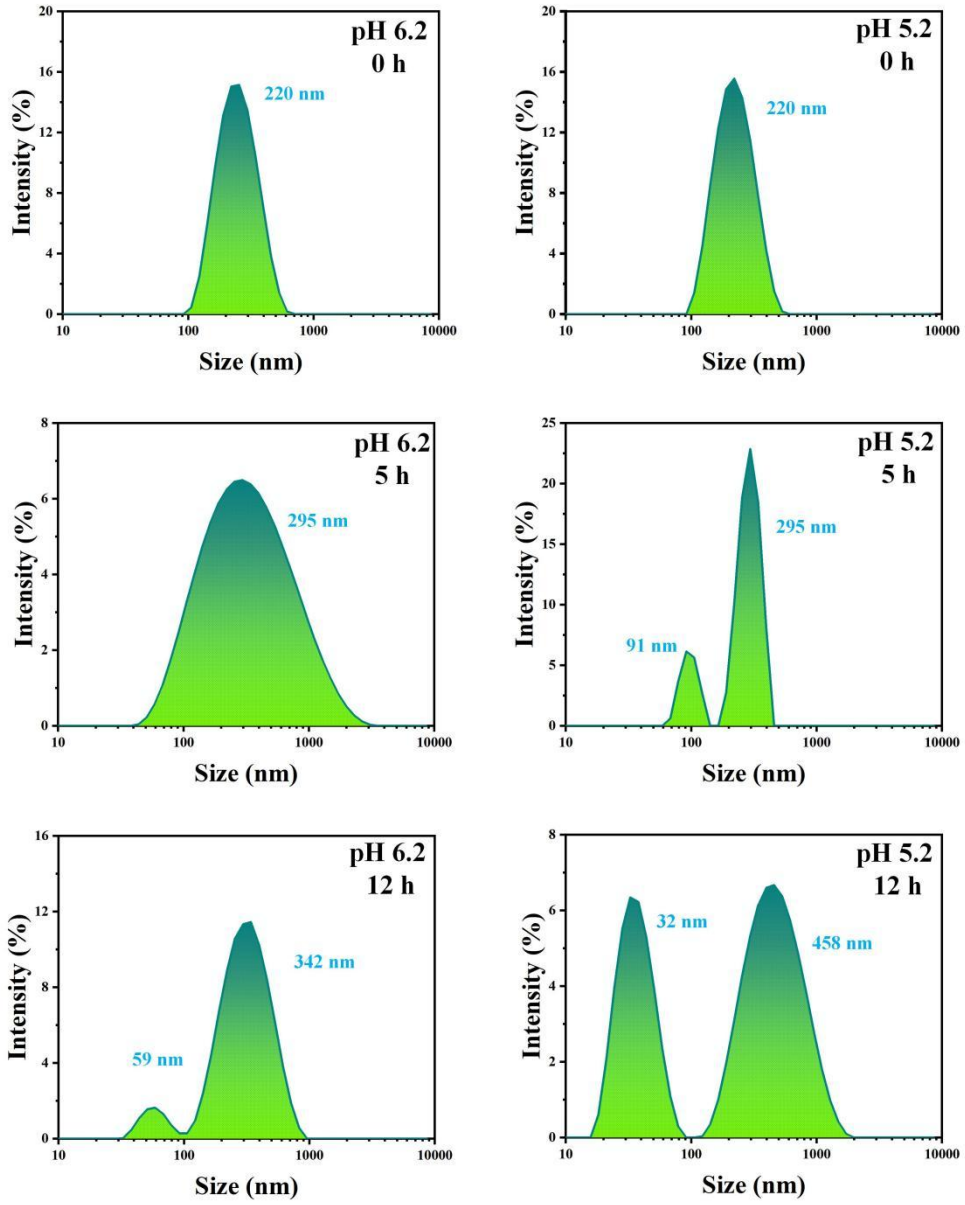

Figure S15. Size distribution changes of GQD NT at different pH values (pH 6.5 and pH 5.2). Typically, the GQD NT were dispersed in neutral PBS, which was then added with 0.1 M HCl solution to adjust the pH values.

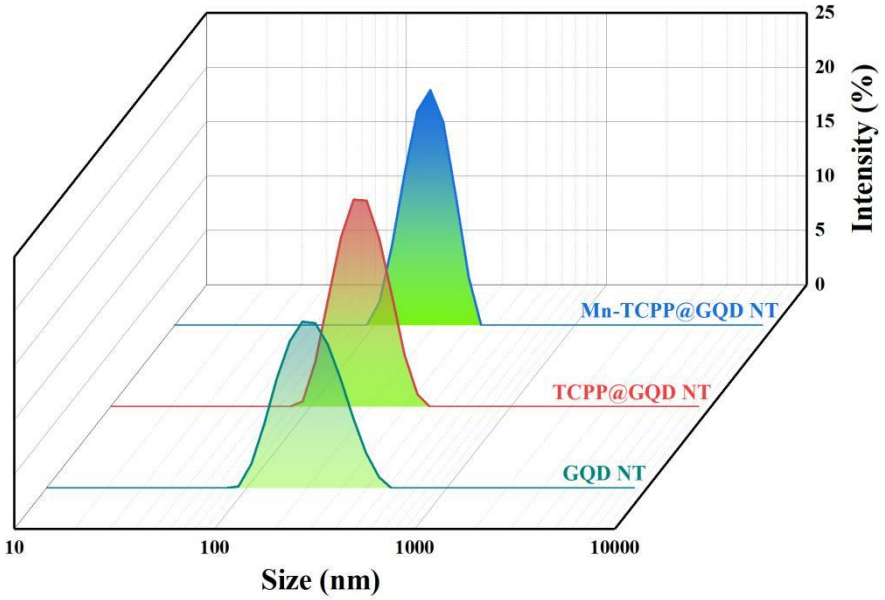

Figure S16. Hydrodynamic size distribution of GQD NT (green), TCPP@GQD NT (red), and Mn-TCPP@GQD NT (blue).

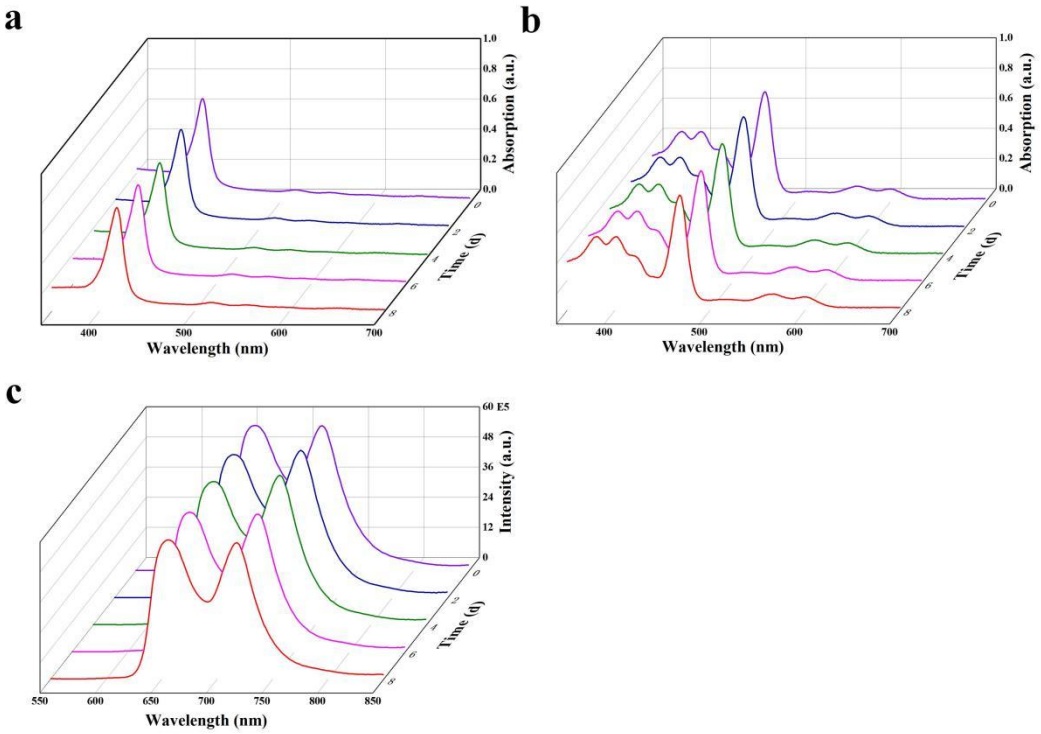

Figure S17. (a) UV-vis spectra of TCPP@GQD NT, (b) UV-vis spectra of Mn-TCPP@GQD NT, and (c) fluorescence spectra of TCPP@GQD NT in PBS (pH 7.4).

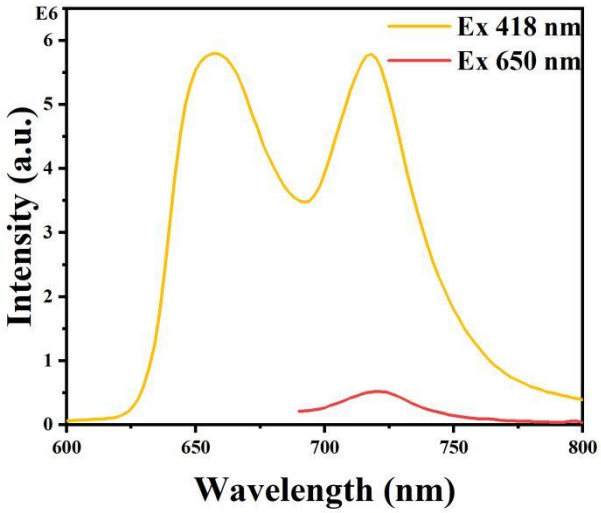

Figure S18. Fluorescence spectra of TCPP@GQD NT.

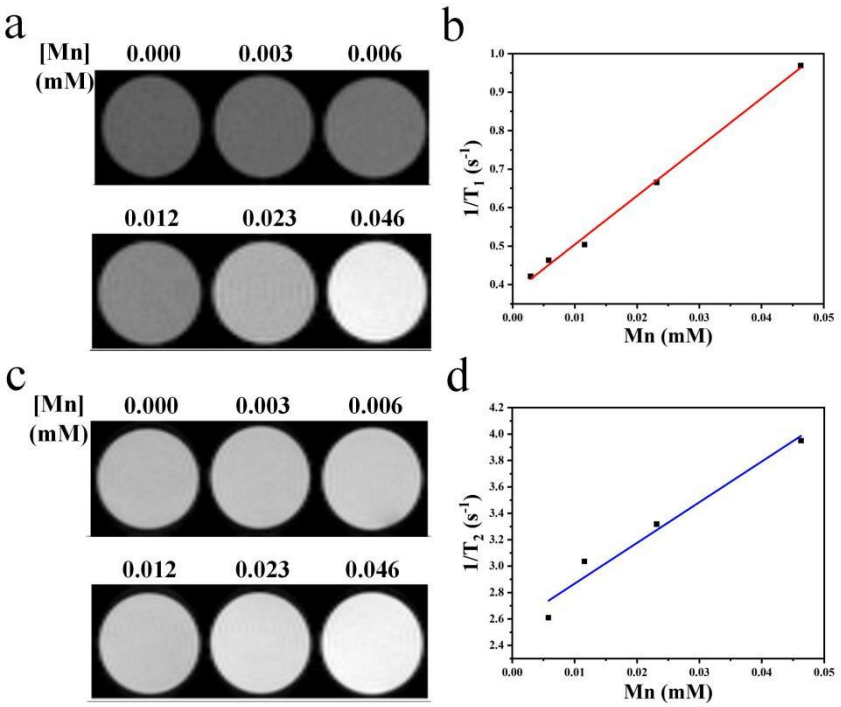

Figure S19. T_1-weighted MRI images (a) and T_1 relaxation rate measurement (b) of Mn-TCPP@GQD NT, and T_2-weighted MRI images (c) and T_2 relaxation rate measurement (d) of Mn-TCPP@GQD NT.

Table S1. Comparison of longitudinal relaxation between Mn-TCPP@GQD NT and small molecule T_1 MRI contrast agents.

Contrast agent	r_1 / $mM^{-1}s^{-1}$	Reference
Gd-DTPA	4.69	[6]
Gd-DOTA	4.74	[6]
Mn-TCPPNa_4	5.10	[1]
Mn-DPDP	2.5	[7]
Mn(EDTA)$(H_2O)^{2-}$	3.0	[8]
Mn(12-pyN_4A)$(H_2O)^{+}$	2.39	[9]
Mn-TCPP@GQD NT	12.65	This work

Cellular Experiments Section

Cell Culture. A549, MRC5, and MCF7 cells were cultured in F12K, MEM, and DMEM respectively. All mediums were supplemented with 10% inactivated fetal bovine serum and 1% penicillin/streptomycin. All cells were cultured at 37 ℃ in a humidified 5% CO_2 atmosphere.

Cytotoxicity Assay. To examine the cytotoxicity of the nanodrug, a 3-[4, 5-dimethylthialzol-2-yl]-2, 5-diphenyltetrazolium bromide (MTT) assay was used. A549 cells were seeded in a 96-well plate at a 5×10^3 per well in 200 μL of media for 12 h, and then treated with GQD NT, TCPP@GQD NT, and Mn-TCPP@GQD NT at different concentrations (0, 50, 100, 150, 200, and 250 μg/mL) of. After 24 h incubation, the medium was replaced with 200 μL MTT (0.5 mg/mL) solution and the cells were incubated for another 4 h. Cells treated with normal medium were used as control. The medium was replaced with 200 μL DMSO and the absorbance values were measured by a microplate reader (SpectraMax 190, Molecular Devices). All the experiments were conducted three times.

For cellular phototoxicity, A549 cells were seeded in a 96-well plate and incubated with GQD NT and TCPP@GQD NT for 4 h. The TCPP@GQD NT groups were irradiated with a 650 nm laser (100 mW/cm^2; 2 min, 4 min, 6min, 8 min, and 10 min). The cell viability was measured by the MTT assay.

Cellular Uptake. For the cellular uptake, MRC5 cells, MCF7 cells, and A549 cells at a density of 2×10^5 were cultured in a 6-well plate with a coverslip for 12 h. TCPP@GQD NT (150 μg/mL) was added and cells were incubated for 1 h. Then, cells were washed with 5% DMSO/PBS solution, fixed with 4% paraformaldehyde, and stained with DAPI. Finally, cells were directly observed by a laser scanning confocal microscope after coverslip was mounted on slides in fluoromount. For the cellular uptake at different pH environments, cells were

treated with solution of TCPP@GQD NT with different pH (pH 6.2, 6.8, and 7.4) for 1 h. HCl (0.1 M) and NaOH (0.1 M) were used to adjust the pH of the culture medium.

3D Cell Culture Imaging. A549 cells were plated in U bottom ultralow attachment 96-well plates at a density of 1×10^5 cells per well and cultured for 3 days with 200 μL F12K (10% FBS). Then, the medium was replaced with 100 μL solution of the naodrugs and incubated for the appropriate time. Respectively, the incubation time was 2 h for TCPP@GQD NT (RGD+) /TCPP@GQD NT (RGD-) group and 1 h for TCPP@GQD NT (pH 7.4, 6.8, 6.2) group. After discarding the supernatant, the 3D cell cultures were washed gently with PBS and transferred to 35 mm glass bottom cell culture dish. Images were captured using a confocal laser scanning microscope with XYZ imaging model (488 nm excitation, 2 μm Z axis step size).

Detection of Singlet Oxygen *In Vitro*. A549 cells at a density of 2×10^5 were seeded in a 6-well plate with a coverslip for 12 h and incubated with GQD, GQD NT, and TCPP@GQD NT (150 μg/mL, same GQD concentration as GQD and GQD NT group) for 4 h. After washing with 5% DMSO/PBS solution, cells were incubated with singlet oxygen detection agent for 2 h, then washed with PBS and irradiated with 650 nm laser at a power density of 100 mW/cm^2 for 10 min. After 4% paraformaldehyde fixation and mounted coverslip on slides in fluoromount, cells were directly imaged under a laser scanning confocal microscope.

Calcien AM/PI Staining. A549 cells were cultured in a 6-well plate with a coverslip at a density of 2×10^5 for 12 h. Then, the medium was replaced with 2 mL fresh F12K containing GQD, GQD NT, and TCPP@GQD NT (150 μg/mL, same GQD concentration as GQD and GQD NT group) respectively. After incubation for another 4 h, cells were washed with 5% DMSO/PBS solution and irradiated with 650 nm laser at a power density of 100 mW/cm^2 for 10 min per well. The cells of each group were stained with calcein AM and PI, triply rinsed with PBS. After 4% paraformaldehyde fixation and mounted coverslip on slides in fluoromount, cells were directly imaged under a laser scanning confocal microscope.

Cell Apoptosis Assay. A549 cells were cultured 6-well plate with a coverslip at a density of 2 × 10^5 cells/well for 12 h. Then, the medium was replaced with 2 mL fresh F12K containing GQDs, GQD NT, and TCPP@GQD NT (150 μg/mL, same GQD concentration as GQD and GQD NT group) respectively. After incubation for another 4 h, cells were washed with 5% DMSO/PBS solution and irradiated with a 650 nm laser at a power density of 100 mW/cm^2 for 10 min. The apoptosis of cells was evaluated by using Annexin V-fluo647/PI apoptosis detection kit. The cells of each group were stained with Annexin V-fluo647 and PI, triply rinsed with PBS. After 4% paraformaldehyde fixation and mounted coverslip on slides in fluoromount, cells were directly imaged under a laser scanning confocal microscope.

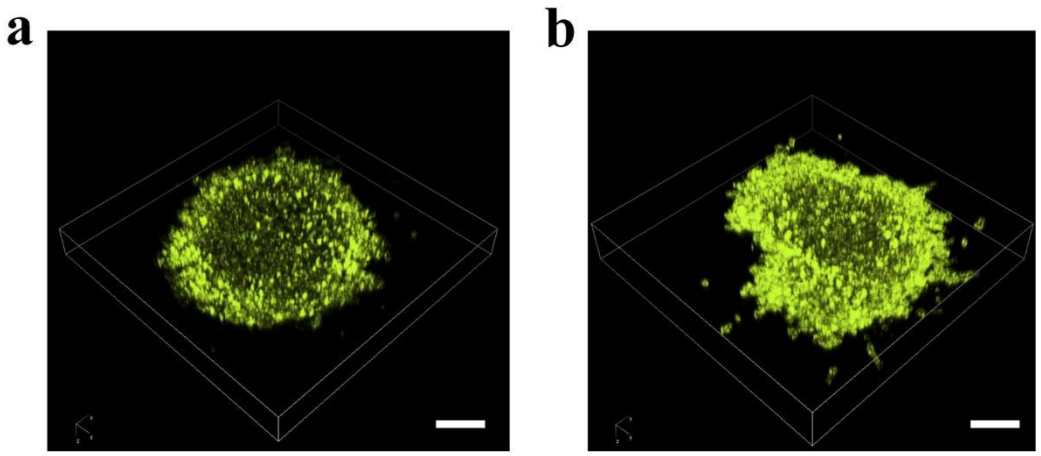

Figure S20. 3D confocal laser scanning microscope (CLSM) imaging results showed the penetration of (a) TCPP@GQD NT (RGD-) and (b) TCPP@GQD NT (RGD+) in A549 3D cell spheroids. Scale bar, 200 μm.

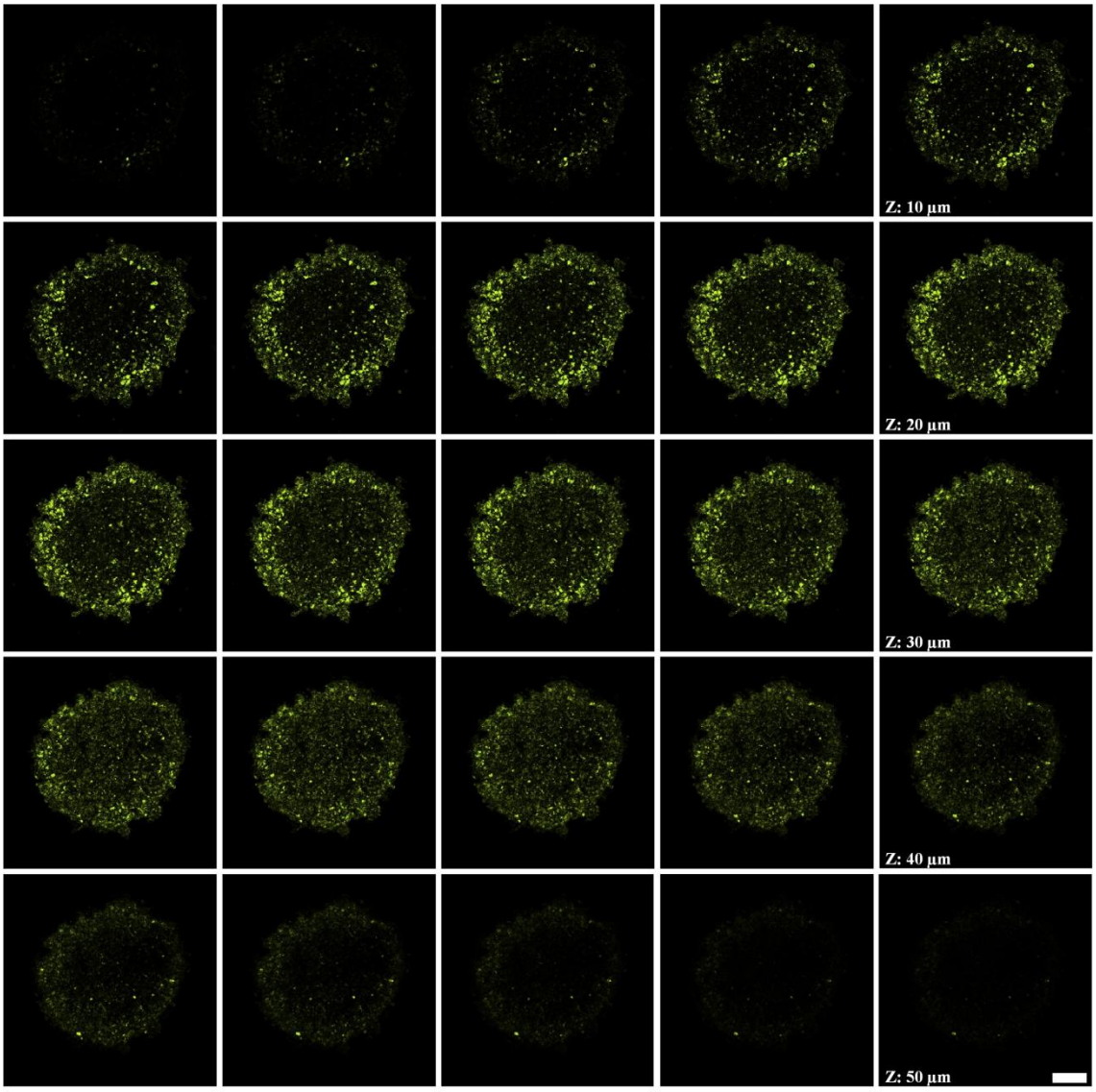

Figure S21. CLSM imaging of A549 3D cell spheroids after TCPP@GQD NT (RGD-) treatment. Scale bar, 200 μm. Z step size, 2 μm.

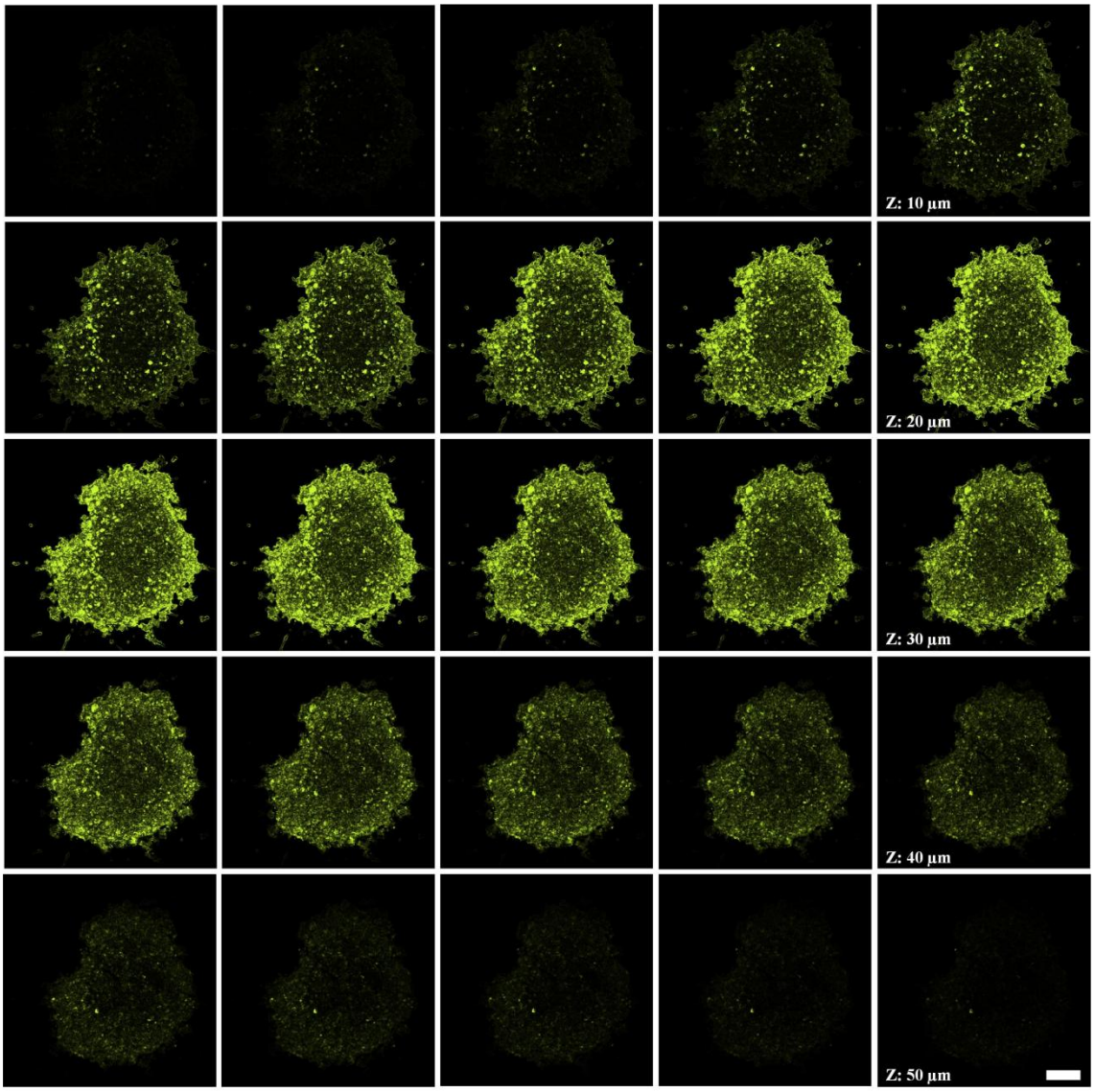

Figure S22. CLSM imaging of A549 3D cell spheroids after TCPP@GQD NT (RGD+) treatment. Scale bar, 200 μm. Z step size, 2 μm.

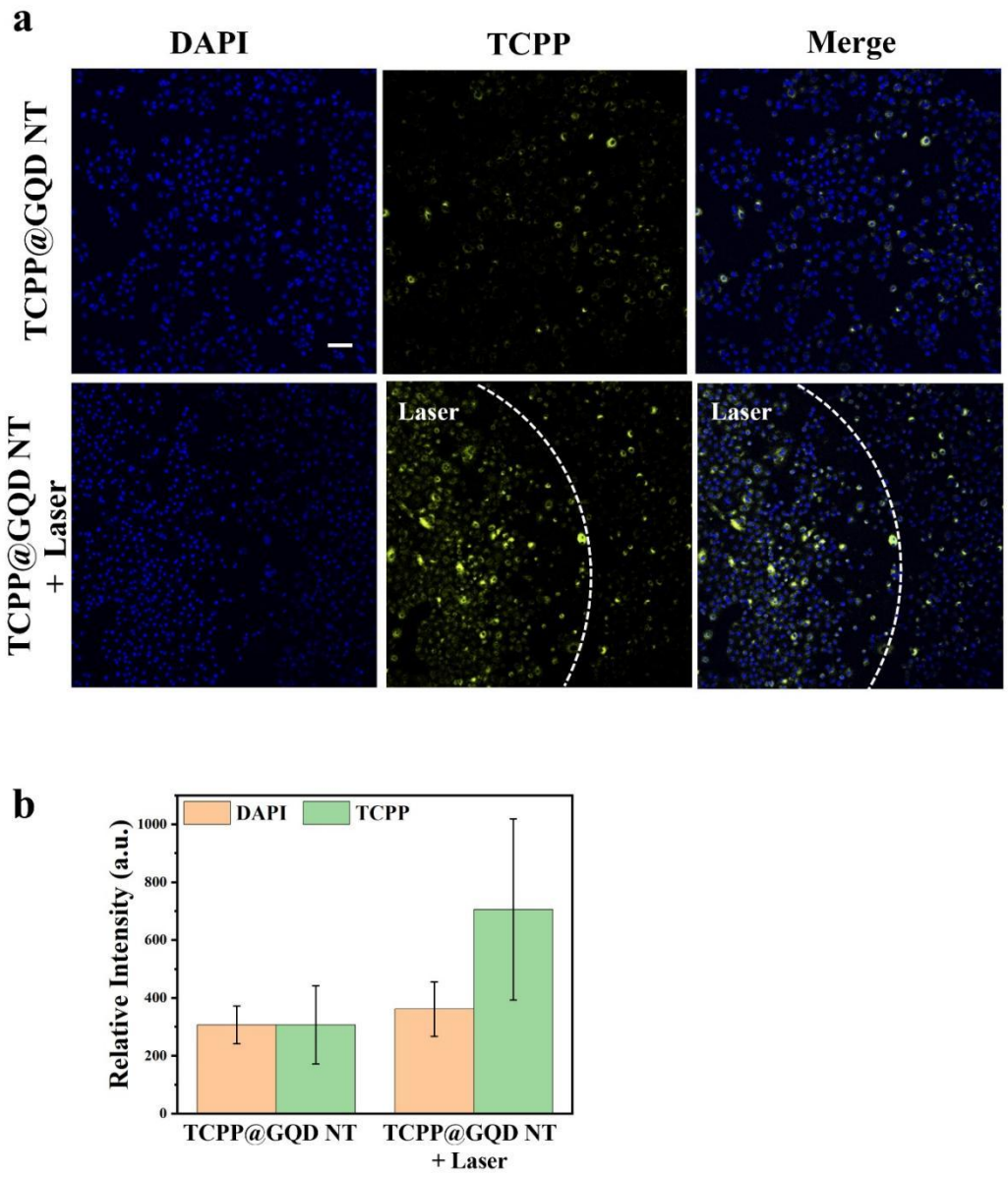

Figure S23. Mild photothermal effect enhanced the cellular uptake of the nanodrug. (a) CLSM images of cells treated with TCPP@GQD NT and laser irradiation. Scale bar, 100 μm. (b) Quantitative analysis of the fluorescence (FL) intensity of TCPP@GQD NT in irradiated and unirradiated areas.

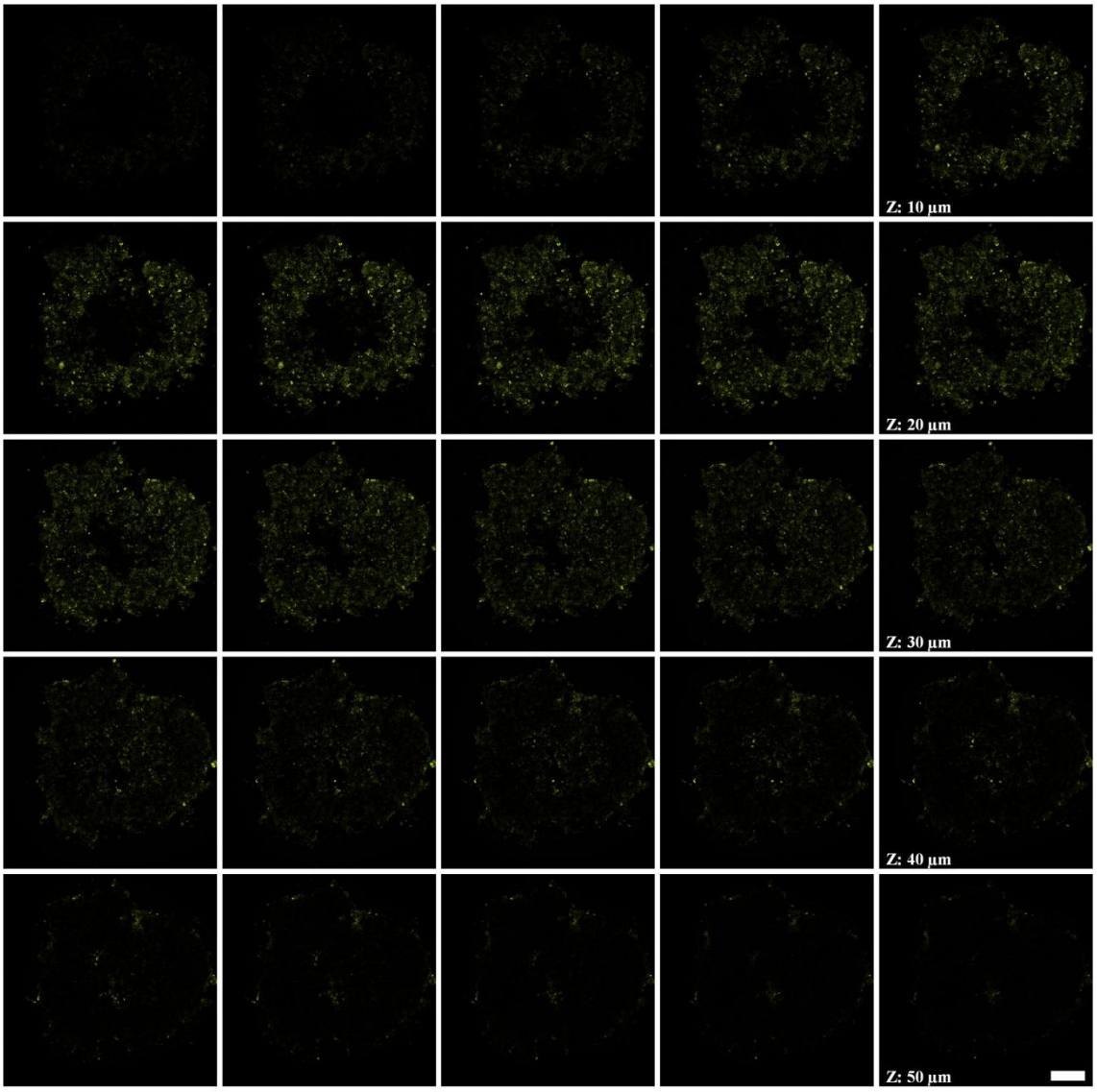

Figure S24. CLSM imaging of A549 3D cell spheroids after TCPP@GQD NT (pH 7.4) treatment. Scale bar, 200 µm. Z step size, 2 µm.

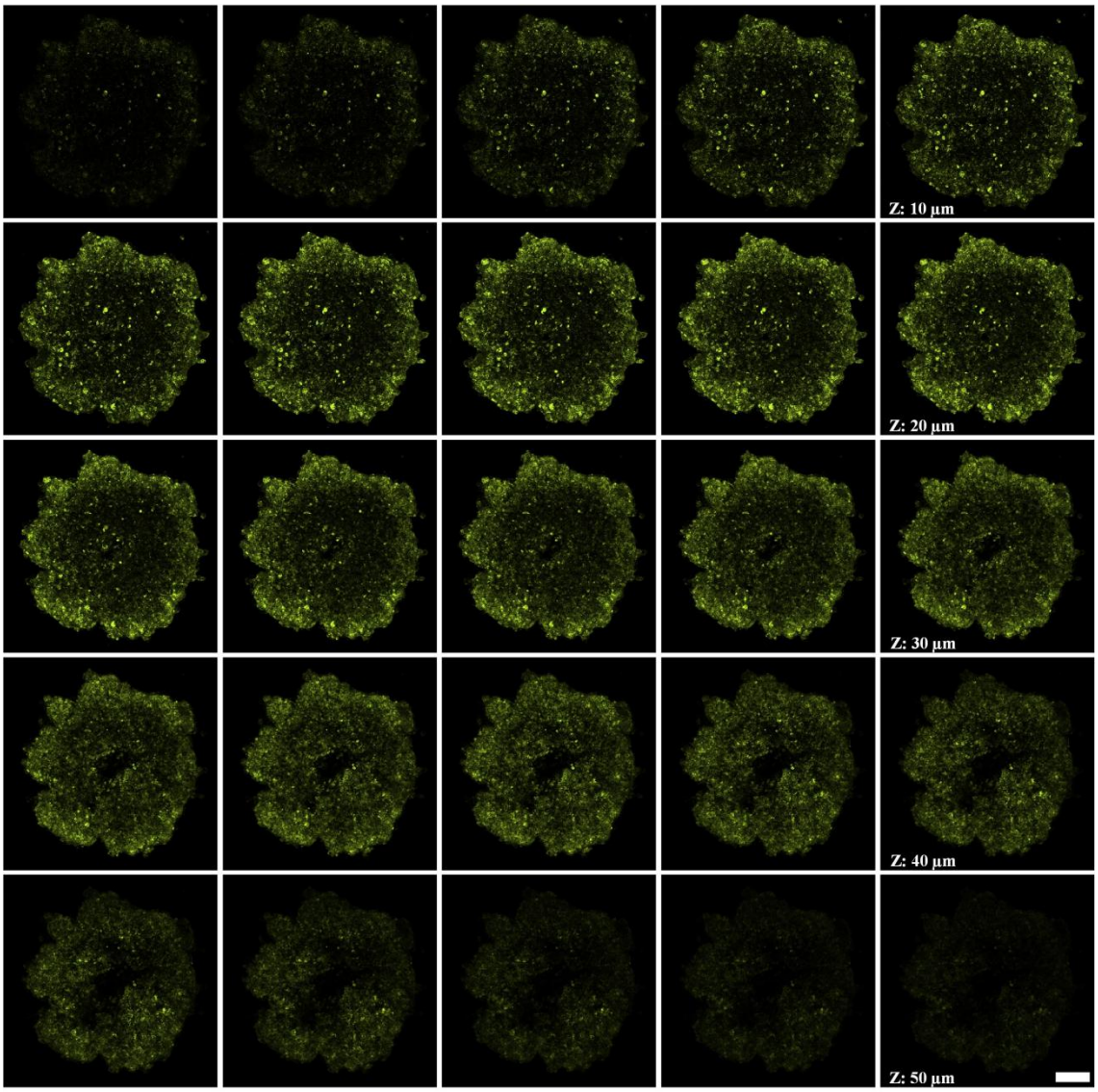

Figure S25. CLSM imaging of A549 3D cell spheroids after TCPP@GQD NT (pH 6.8) treatment. Scale bar, 200 µm. Z step size, 2 µm.

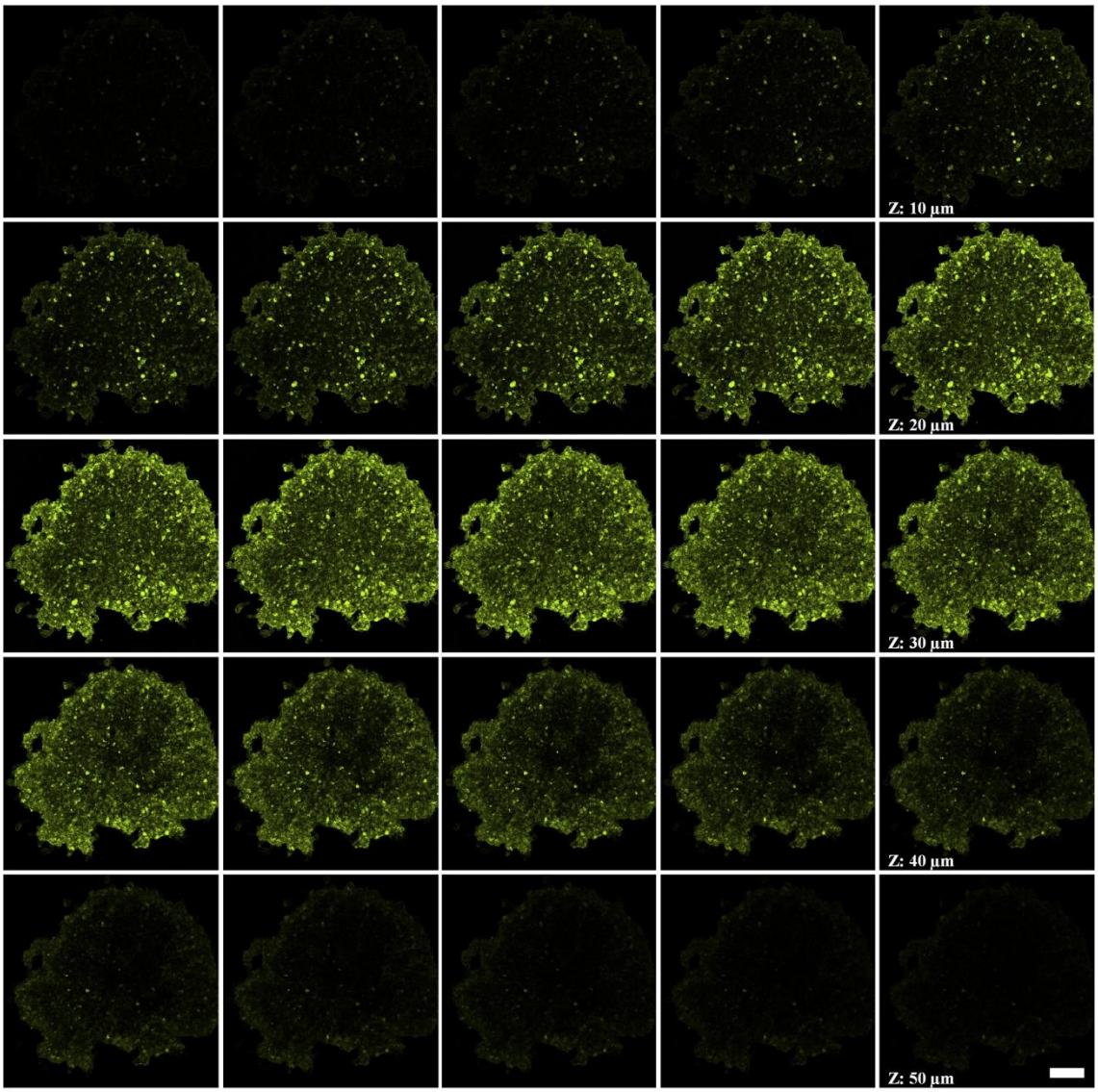

Figure S26. CLSM imaging of A549 3D cell spheroids after TCPP@GQD NT (pH 6.2) treatment. Scale bar, 200 µm. Z step size, 2 µm.

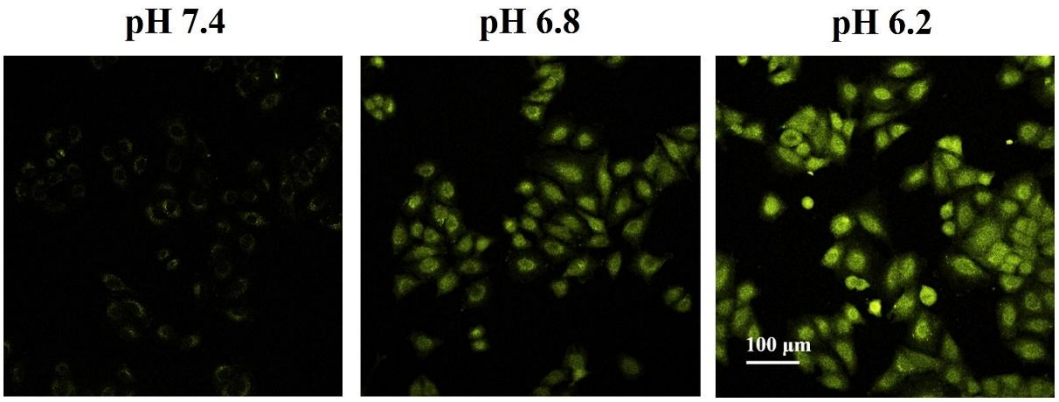

Figure S27. Acidity triggered the recovery of fluorescence from TCPP. A549 cells were incubated with 150 μg/mL TCPP@GQD NT in pH 6.2, 6.8 and 7.4 buffers, respectively. Scale bar, 100 μm. Quantitative analysis of the fluorescence (FL) intensity is shown in the maintext, Figure 2d.

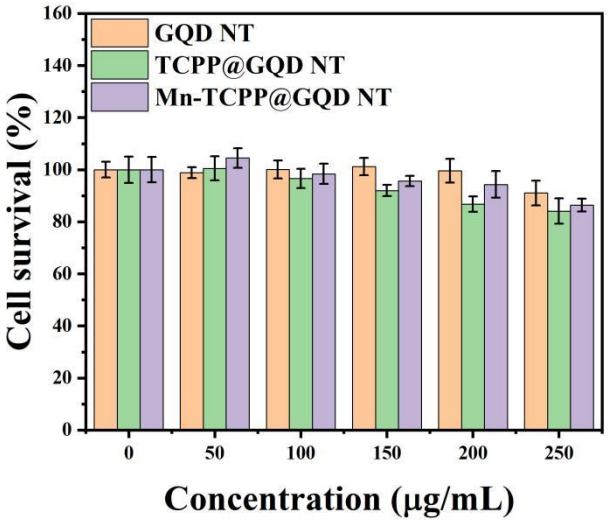

Figure S28. Cell viabilities of A549 cells treated with GQD NT, TCPP@GQD NT and Mn-TCPP@GQD NT at different concentrations for 24 h.

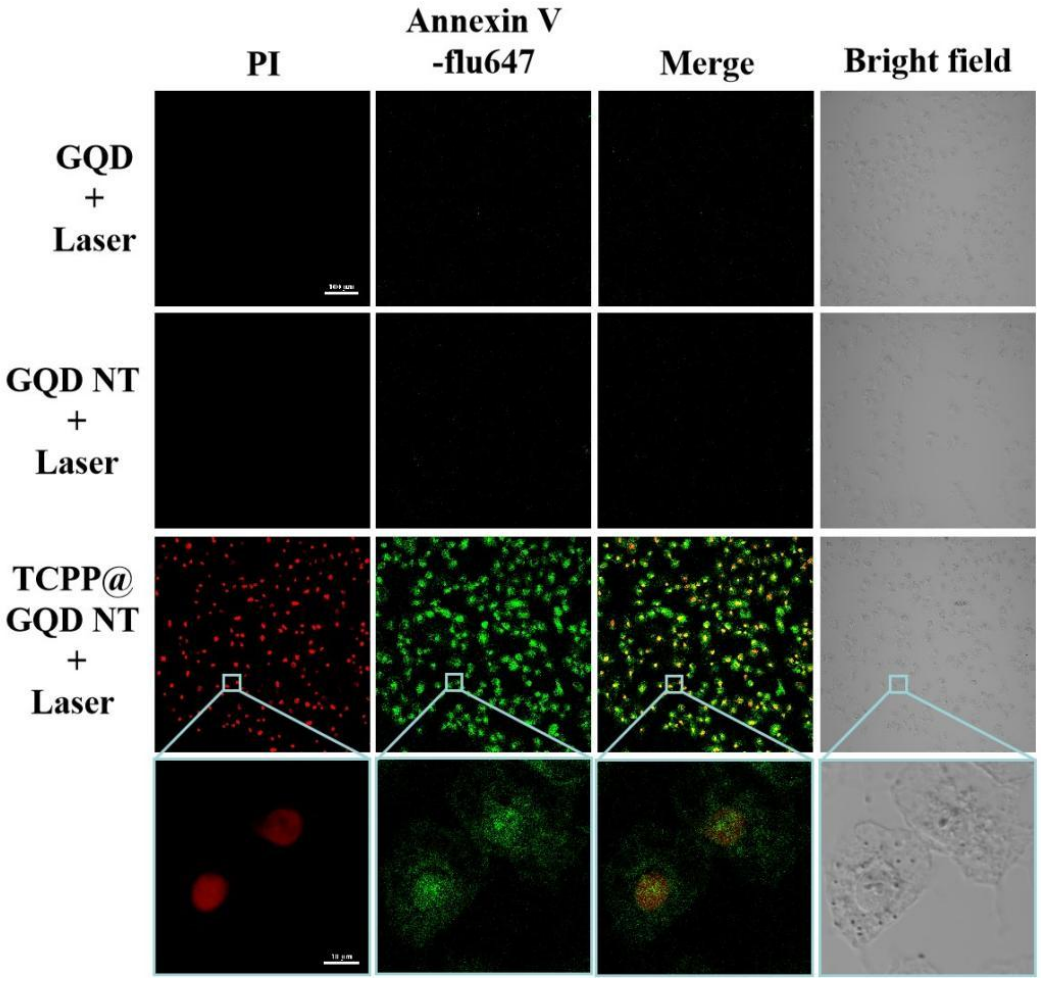

Figure S29. Annexin-V/PI double staining assay for evaluating the apoptosis of A549 cells. The membrane of apoptotic cells were dyed to green, and the nuclei of apoptotic cells were dyed to red. Scale bar, 100 μm and 10 μm (zoom in).

***In Vivo* Experiments Section**

Tumor Implantation. The Balb/c nude mice (4-5 weeks of age, 18-20 g, male) were purchased from Vital River Laboratory Animal Technology Co. Ltd (Beijing, China). The mice were housed in a specific pathogen-free (SPF) laboratory under conditions of 23 ℃, 40-50% humidity, and a 12 h light/dark cycle. The animal procedures and experiments were approved by the Ethics Committee for Animal Research, Innovation Academy for Precision Measurement Science and Technology, Chinese Academy of Sciences. To induce a tumor, 2 × 10^7 A549 cells were suspended in 200 μL PBS and injected subcutaneously into the right hind leg of mice.

***In Vivo* and *ex Vivo* Fluorescence Imaging.** To investigate the *in vivo* targeting ability, TCPP@GQD NT (3 mg, 200 μL, containing 0.22 μmol TCPP) with or without RGD were intravenously injected into A549 tumor-bearing nude mice. Then, fluorescent scans were recorded on an IVIS system (λ_{ex} 640 nm, λ_{em} 720 nm) to observe the *in vivo* distribution of TCPP@GQD NT at different injection times. The mice were executed and the major organs were collected for fluorescence imaging after 72 h or 96 h. For *ex vivo* fluorescence imaging, the TCPP@GQD NT-injected mice were sacrificed at different post-injection (*p.i.*) time points. Their major organs (hearts, livers, spleens, lungs, and kidneys) were excised for fluorescence imaging.

Tumor Slice Observation. To confirm the *in situ* morphologic change of the GQD NT in tumor tissues, A549 tumor-bearing mice were intravenously injected with GQD NT (3 mg, 200 μL). For comparison, the mice treated with PBS were set as the control group. For biological TEM (bio-TEM) observation, these mice were sacrificed at 4 h and 24 h *p.i.*. Their tumor tisssues were excised and fixed in 2.5% glutaraldehyde solutions. For CLSM imaging, A549 tumor-bearing mice were intravenously injected with TCPP@GQD NT or TCPP@GQD. These mice were sacrificed at 24 h *p.i.*. Their tumor tissues were excised and

fixed in 4% paraformaldehyde solutions. All tumor slices and staining experiments were conducted by a biological company (Servicebio Technology Co., Ltd., Wuhan). Tumor slice images were captured using a confocal laser scanning microscope (DAPI: 405 nm excitation, TCPP: 647 nm excitation)

***In Vivo* Blood Circulation Behavior**. A549 tumor-bearing mice were intravenously injected with TCPP@GQD NT (3 mg, 200 μL) suspension. The blood samples were collected from the mice at the specific time points (10 min, 30 min, 1 h, 2 h, 4 h, 8 h, 12 h, and 24 h) and separated plasma. Finally, the TCPP content in the plasma samples was measured by microplate reader.

***In Vivo* T_1-weight MRI.** A549 tumor-bearing nude mice were anesthetized with 4% isoflurane/oxygen, and then the Mn-TCPP@GQD NT (6 mg, 200 μL, containing 0.56 μmol Mn-TCPP) was intravenously injected. T_1-weight MRI was performed on 7T Bruker BioSpec 70/20 USR system, and a RARE-T_1 sequence was used with the following parameters: TR = 500 ms, TE = 9 ms, matrix size = 128 × 128, FOV = 40 × 40 mm, slice thickness = 1 mm.

***In Vivo* Photodynamic Therapy.** A549 tumor-bearing mice were sorted into 6 groups with the following treatments: (1) Saline; (2) Saline + laser; (3) GQD NT + laser; (4) TCPP@GQD NT (0.6 mg, 200 μL, containing 44 nmol TCPP); (5) TCPP@GQD NT + laser, and (6) (TCPP@GQD NT + laser) × 2. The tumor-bearing mice of all groups were anesthetized with 2% isoflurane/oxygen and intravenously injected with saline or different nanoparticle formulations at day 0. Tumor areas were exposed to a 650 nm laser with power of 100 mW/cm^2 for 10 min at 6h, 12h, 24h, and 36h after injection. Group (6) repeated one PDT treatment on day 6. Body weights and tumor sizes of the mice were monitored every three day. The tumor volumes were calculated as follow:

$$\text{Tumor volume (mm}^3\text{)} = 0.5 \times \text{width}^2\ \text{(mm}^2\text{)} \times \text{length (mm)}.$$

***Ex Vivo* Histological Staining and Blood Analysis.** Biocompatibility and tumor inhibition analyses were carried out after the PDT process. The major organs (heart, liver, spleen, lung, and kidney) were collected and fixed with paraformaldehyde and cryosectioned for hematoxylin-eosin (H&E) staining. The blood samples were collected for blood routine and blood biochemistry analysis. The mice treated with saline were used as control. The histological changes of tumor tissues and *in situ* cancer cell apoptotic levels were evaluated by using hematoxylin-eosin (H&E) staining and a terminal-deoxynucleotidyl transferase mediated dUTP-biotin nick end labeling (TUNEL) staining. The proliferative capacity of the tumors was estimated by Ki67 immunohistochemistry assays. All staining experiments were conducted by a biological company (Servicebio Technology Co., Ltd., Wuhan).

Statistical Analysis. The quantitative data were presented as mean ± standard deviation (s.d.) and analyzed with a one-way analysis of variance (ANOVA). Statistical analyses were performed with a two-tailed Student's t-test for experiments with two groups. For all tests, the p values < 0.05 were considered statistically significant ($^{*}p < 0.05$, $^{**}p < 0.01$, $^{***}p < 0.001$, $^{****}p < 0.0001$).

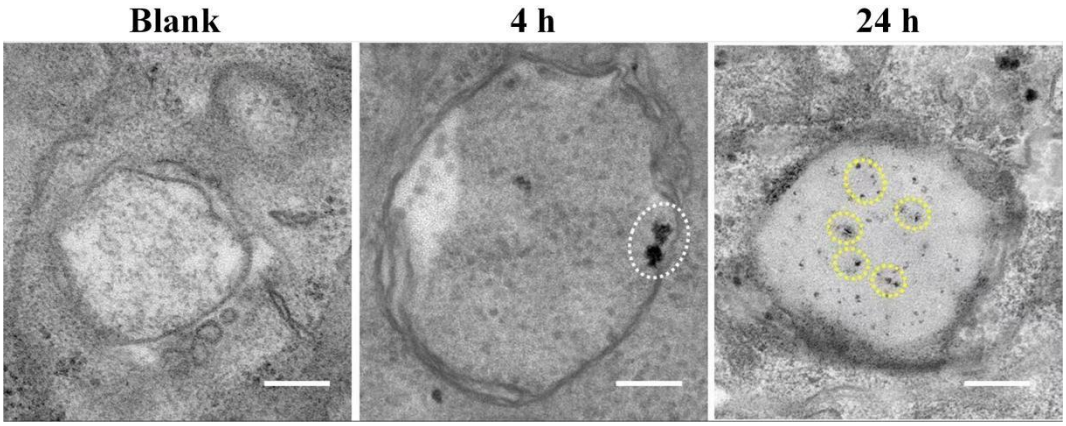

Figure S30. Representative bio-TEM images of tumor slices from the mice that were sacrificed at 4 h and 24 h after *i.v.* injection of the GQD NT. The white area indicated the presence of large size GQD NT in lysosomes after 4 h *i.v.* injection. The yellow area indicated the presence of small size GQD NT in lysosomes after 24 h *i.v.* injection. Scale bar, 200 nm.

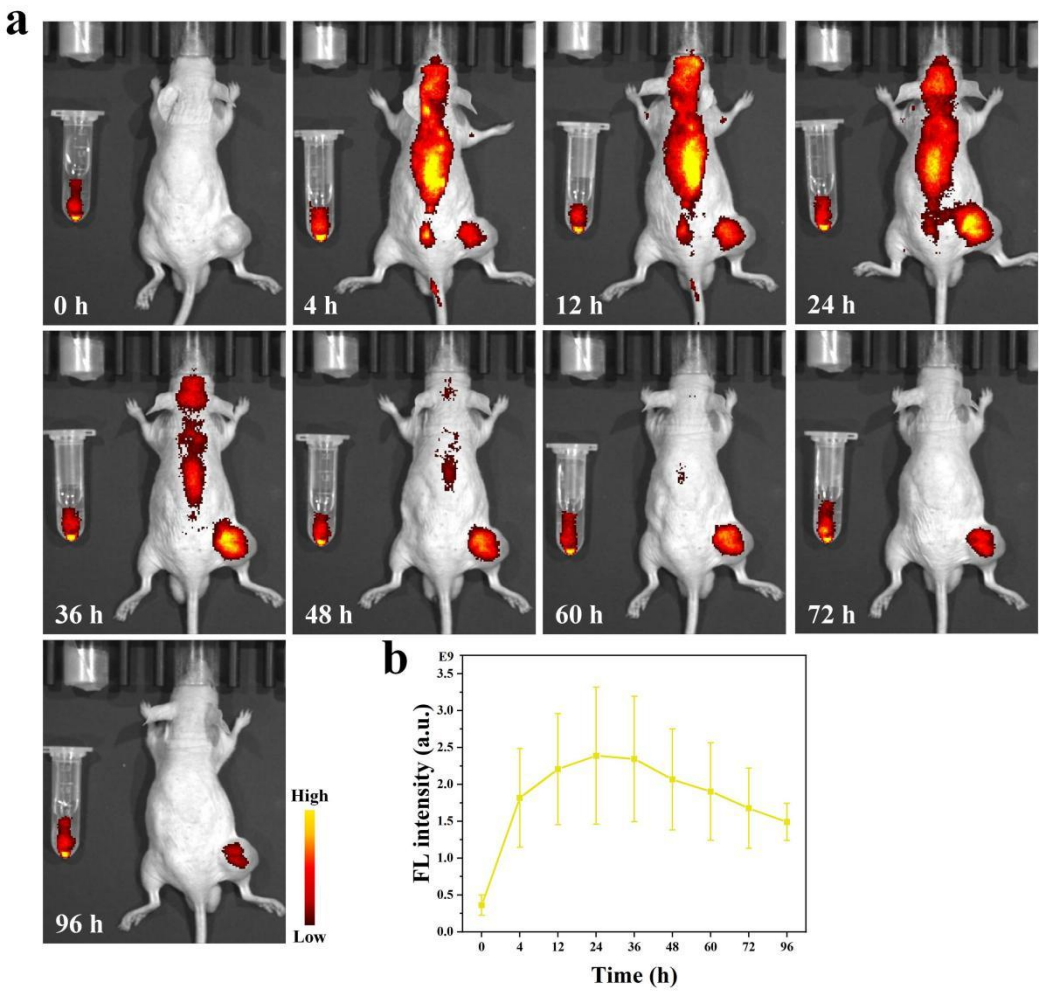

Figure S31. (a) Fluorescence imaging and (b) Fluorescence intensity measurements of tumors after intravenous injection of TCPP@GQD NT at various times (n = 3).

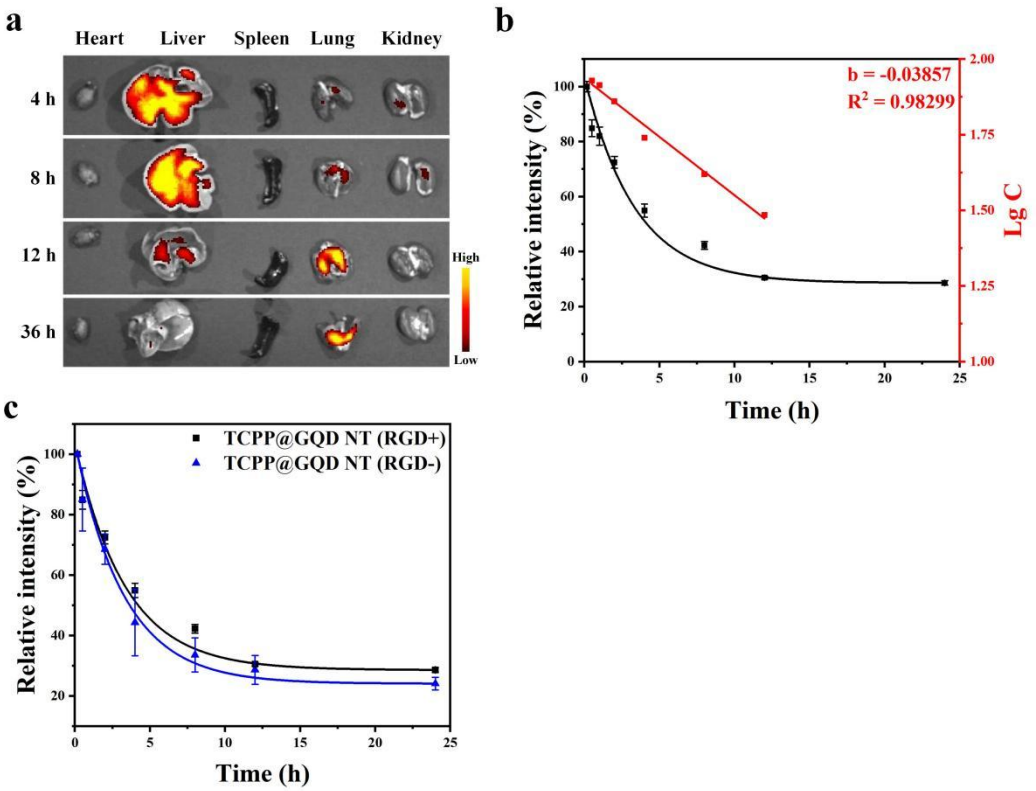

Figure S32. Biodistribution and metabolism of TCPP@GQD NT. (a) The *ex vivo* organ distribution of TCPP@GQD NT at different time points after *i.v.* injection. Blood circulation behavior (b) of TCPP@GQD NT and (c) TCPP@GQD NT (RGD-) after *i.v.* injection by recording the TCPP UV-vis absorption of plasma sample withdrawn from the injected mice at different time intervals.

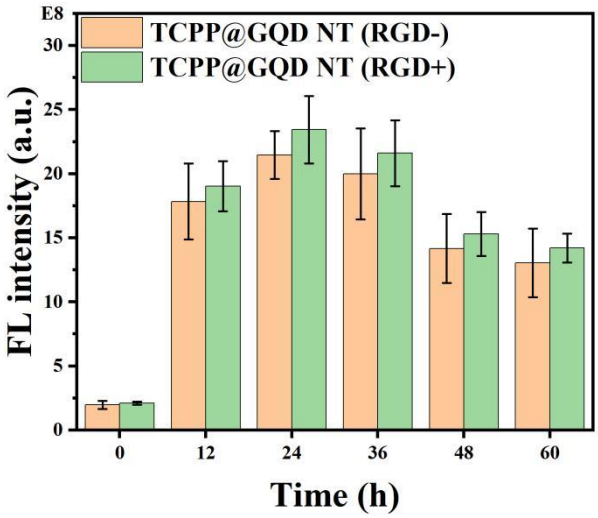

Figure S33. Fluorescence intensity measurements of tumors after intravenous injection of TCPP@GQD NT (RGD+) and TCPP@GQD NT (RGD-) at various times.

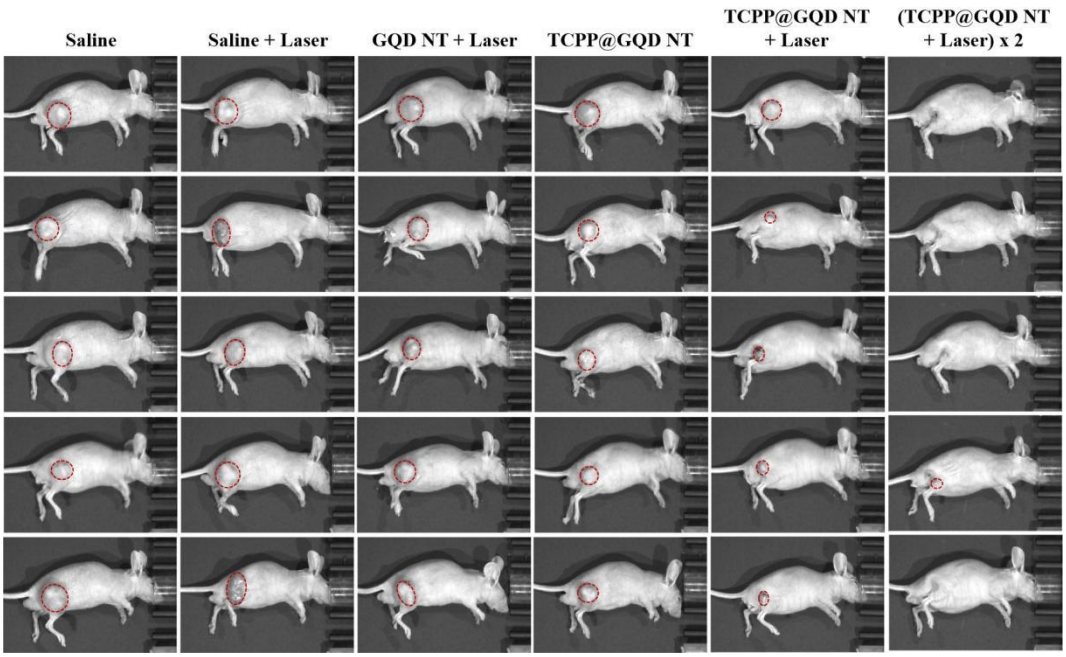

Figure S34. Digital photos of mice after PDT treatments. Tumor area is circled with red dashed line.

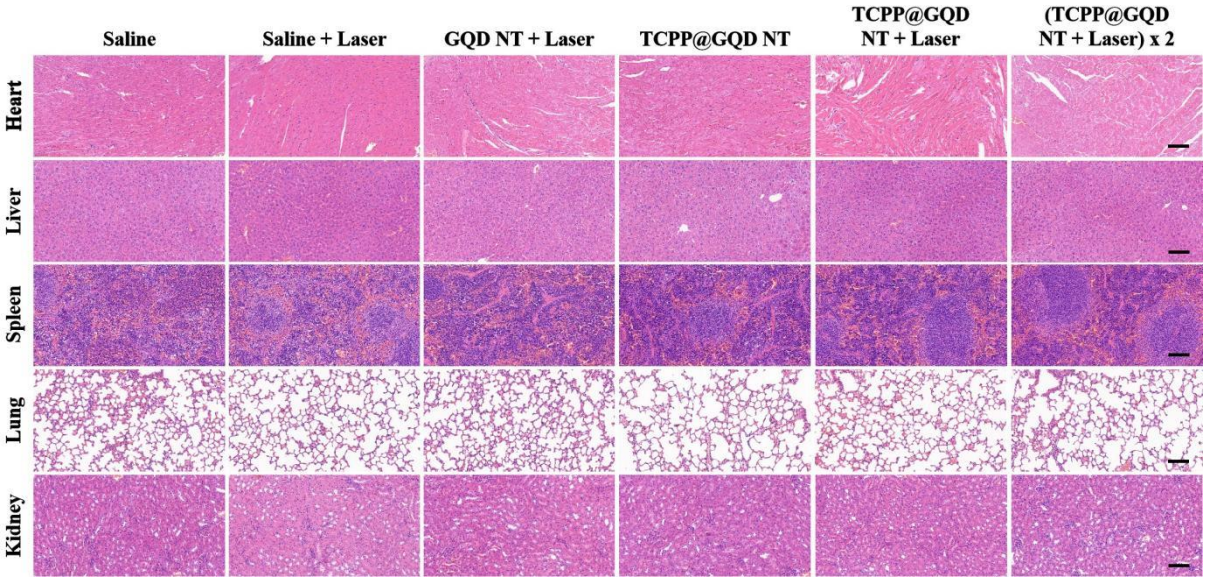

Figure S35. H&E staining of major organs after different treatments. Scale bar, 100 μm.

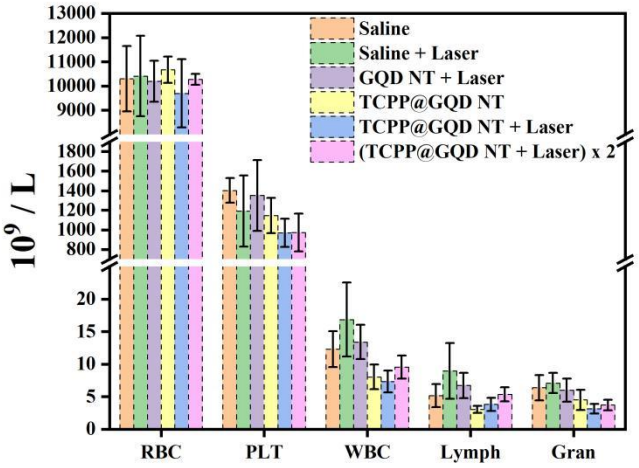

Figure S36. Main blood cells concentration of RBC, PLT, WBC, Lymph, and Gran after different treatments.

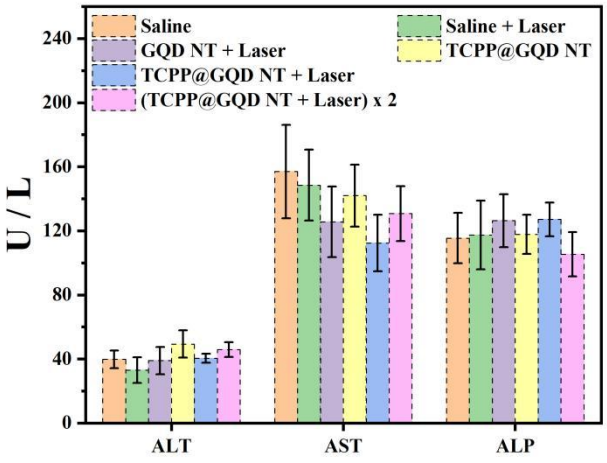

Figure S37. Liver function-related enzymes concentration of ALT, AST, and ALP after different treatments.

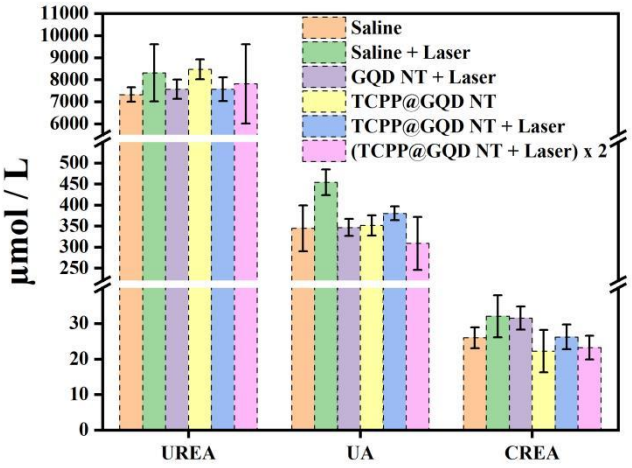

Figure S38. Kidney function-related substrates concentration of UREA, CREA, and UA after different treatments.

Table S2. Comparison of laser powers and drug doses for repeated PDT strategies.

	Photosensitizer	Single drug dose [a)]	Number of injections	Single laser power	Number of irradiation	Injection method	Total dose	
							Drug	Irradiation
Small molecules	Ce6 [10]	2 mg/kg (3.35 μmol/kg)	6	300 J/cm^2	6	Intravenous injection	20.1 μmol/kg	1800 J/cm^2
	IR820 [10]	8 mg/kg (9.67 μmol/kg)	6	300 J/cm^2	6	Intravenous injection	58.0 μmol/kg	1800J/cm^2
	Ce6 [11]	4 mg/kg (6.70 μmol/kg)	7	60 J/cm^2	14	Intravenous injection	46.9 μmol/kg	840 J/cm^2
Nanoparticles	Ppa-iRGDC-BK01 (PPa) [12]	10 nmol (0.4 μmol/kg)	1	120 J/cm^2	5	Peritumoral injection	0.4 μmol/kg	600 J/cm^2
	T820/Ce6 micelles (IR820, Ce6) [10]	10 mg/kg (13.02 μmol/kg)	6	300 J/cm^2	6	Intravenous injection	78.1 μmol/kg	1800 J/cm^2
	GCZ@M (Ce6) [13]	10 mg/kg (16.76 μmol/kg)	2	900 J/cm^2	3	Intravenous injection	33.5 μmol/kg	2700 J/cm^2
	Sm-TCPP (TCPP) [14]	7.9 mg/kg (10 μmol/kg)	4	90 J/cm^2	4	Intravenous injection	40 μmol/kg	360 J/cm^2
	Fe_3O_4@DexTPP/ PpIX/ss-mPEG (PpIX) [15]	5 mg/kg (8.89 μmol/kg)	4	60 J/cm^2	4	Intravenous injection	35.5 μmol/kg	240 J/cm^2
	LMAC (Ce6) [16]	20 mg/kg (33.52 μmol/kg)	3	225 J/cm^2	3	Intravenous injection	100.6 μmol/kg	675 J/cm^2
	GQD NT [This work] (TCPP)	44 nmol (1.76 μmol/kg)	2	60 J/cm^2	8	Intravenous injection	3.5 μmol/kg	480 J/cm^2

[a)] For nanoparticles, the comparison of drug doses was carried out by converting nanoparticle doses into small molecule PS doses.

References

[1] Y. Liu, Y. Huang, P. O. Boamah, Q. Zhang, Y. Liu, M. Hua, *Chem. Res. Chin. Univ.* **2014**, *30*, 549.

[2] Y. Yang, S. Chen, L. Liu, S. Li, Q. Zeng, X. Zhao, H. Li, Z. Zhang, L. S. Bouchard, M. Liu, X. Zhou, *ACS Appl. Mater. Interfaces* **2017**, *9*, 23400.

[3] R. C. Petter, J. S. Salek, C. T. Sikorski, G. Kumaravel, F. T. Lin, *J. Am. Chem. Soc.* **1990**, *112*, 3860.

[4] J. Liu, W. E. Hennink, M. J. van Steenbergen, R. Zhuo, X. Jiang, *J. Mater. Chem. B* **2016**, *4*, 7022.

[5] H. Wang, S. Wang, H. Su, K. J. Chen, A. L. Armijo, W. Y. Lin, Y. Wang, J. Sun, K. Kamei, J. Czernin, C. G. Radu, H. R. Tseng, *Angew. Chem. Int. Ed.* **2009**, *48*, 4344.

[6] D. H. Powell, O. M. N. Dhubhghaill, D. Pubanz, L. Helm, Y. S. Lebedev, W. Schlaepfer, A. E. Merbach, *J. Am. Chem. Soc.* **1996**, *118*, 9333.

[7] B. Gallez, G. Bacic, H. M. Swartz, *Magn. Reson. Med.* **1996**, *35*, 14.

[8] J. Maigut, R. Meier, A. Zahl, R. van Eldik, *J. Am. Chem. Soc.* **2008**, *130*, 14556.

[9] B. Drahoš, J. Kotek, I. Císařová, P. Hermann, L. Helm, I. Lukeš, É. Tóth, *Inorg. Chem.* **2011**, *50*, 12785.

[10] X. Hu, H. Tian, W. Jiang, A. Song, Z. Li, Y. Luan, *Small* **2018**, *14*, 1802994.

[11] C. Zhang, C. Li, Y. Li, J. Zhang, C. Bao, S. Liang, Q. Wang, Y. Yang, H. Fu, K. Wang, D. Cui, *Adv. Funct. Mater.* **2015**, *25*, 1314.

[12] H. J. Cho, S. J. Park, W. H. Jung, Y. Cho, D. J. Ahn, Y. S. Lee, S. Kim, *ACS Nano* **2020**, *14*, 15793.

[13] J. An, Y. G. Hu, C. Li, X. L. Hou, K. Cheng, B. Zhang, R. Y. Zhang, D. Y. Li, S. J. Liu, B. Liu, D. Zhu, Y. D. Zhao, *Biomaterials* **2020**, *230*, 119636.

[14] Z. Gao, Y. Li, Y. Zhang, K. Cheng, P. An, F. Chen, J. Chen, C. You, Q. Zhu, B. Sun, *ACS Appl. Mater. Interfaces* **2020**, *12*, 1963.

[15] H. Hou, X. Huang, G. Wei, F. Xu, Y. Wang, S. Zhou, *ACS Appl. Mater. Interfaces* **2019**, *11*, 29579.

[16] F. Gao, W. Zheng, L. Gao, P. Cai, R. Liu, Y. Wang, Q. Yuan, Y. Zhao, X. Gao, *Adv. Healthcare Mater.* **2017**, *6*, 1601453.